

UNCLASSIFIED

AD 269 218

*Reproduced
by the*

**ARMED SERVICES TECHNICAL INFORMATION AGENCY
ARLINGTON HALL STATION
ARLINGTON 12, VIRGINIA**



UNCLASSIFIED

DISCLAIMER NOTICE

THIS DOCUMENT IS THE BEST
QUALITY AVAILABLE.

COPY FURNISHED CONTAINED
A SIGNIFICANT NUMBER OF
PAGES WHICH DO NOT
REPRODUCE LEGIBLY.

NOTICE: When government or other drawings, specifications or other data are used for any purpose other than in connection with a definitely related government procurement operation, the U. S. Government thereby incurs no responsibility, nor any obligation whatsoever; and the fact that the Government may have formulated, furnished, or in any way supplied the said drawings, specifications, or other data is not to be regarded by implication or otherwise as in any manner licensing the holder or any other person or corporation, or conveying any rights or permission to manufacture, use or sell any patented invention that may in any way be related thereto.

CATALOGED BY **ASTIA**
AS AD NO. _____

269218

269 218



**EASTMAN KODAK COMPANY
APPARATUS AND OPTICAL DIVISION**

NOX
62-1-4

ASTIA
RESOLVED
JAN 4 1962
TIPDR

December 6, 1961

Copy No. 89

**Final Report
on a
Space Background Study**

Contract DA-30-069-ORD-2803

EK/ARD ED-735

For the

**Army Rocket and Guided Missile Agency
U. S. Army Ordnance Missile Command
Redstone Arsenal, Alabama**

**This research is a part of Project Defender,
Sponsored by the Advanced Research Projects Agency, ARPA,
Order 39-60, Task 12, Paragraph 1**

Submitted by

**Eastman Kodak Company
Apparatus and Optical Division, Lincoln Plant
Rochester, New York**



ABSTRACT

This is a summary report of a two-year effort by the Eastman Kodak Company in cooperation with the Ohio State University Research Foundation to obtain and present astronomical data designed to show the nature and extent of the infrared space background. Emphasis in the first phase of the contract was placed on historical and theoretical considerations of the problem. A summary table of the computed infrared magnitudes of 235 stars in three infrared wavebands is presented, based on the assumption that stars radiate as blackbodies over their entire spectral range.

The second phase of the contract was designed to test the foregoing assumption by observing and measuring in the infrared a number of selected astronomical sources. To this end two infrared photometer systems were designed and constructed by the Eastman Kodak Company and employed on the Perkins and Mount Wilson Observatories' telescopes. The results of the observations made with these photometers over the period from October, 1960 to September, 1961, are presented.

PREPARED BY

Philip E. Barnhart
Ohio State University
Research Foundation

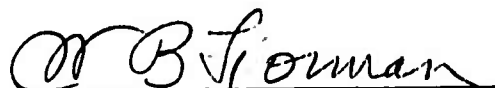
Anthony J. G. Prasil
Eastman Kodak Company

Dr. Walter E. Mitchell, Jr.
Ohio State University
Research Foundation

Charles F. Grams
Eastman Kodak Company

Dr. William H. Haynie
Eastman Kodak Company

SUBMITTED AND APPROVED BY


W. B. Forman, Assistant Director
A & O Research & Engineering

CONTENTS

	<u>Page</u>
Title Page	1
Abstract	3
Signature Page	4
Contents	5
Illustrations	6
References	7
I. Introduction	9
II. Technical Summary	11
III. Technical Approach	14
IV. Instrumentation	18
V. Observing Program	33
Appendix I Notes on Mount Wilson Data Reduction	67
Appendix II Comments on Standard Stars	69
Appendix III The Infrared Characteristics of Protostars and Dark Globules	71
Appendix IV Revised Infrared Star List	85
Appendix V Summary of Stellar Measurements at Perkins Observatory	97
Distribution List	

ILLUSTRATIONS

<u>Figure</u>	<u>Title</u>	<u>Page</u>
1	Infrared Stellar Photometer	20
2	Spectral Characteristics of the Visible-Infrared Dichroic Mirror	21
3	Spectral Response of X Channel	22
4	Spectral Response of Y Channel	23
5	Preamplifier Schematic	25
6	Signal Amplifier and Reference Generator Schematic . . .	26
7	Integrator and Timer Schematic	27
8	The Infrared Photometer System on the Mount Wilson 60-inch Reflector	29
9	Overall View of the Infrared Stellar Photometer System on the Mount Wilson 100-inch Reflector	30
10	Observer at the Visual Tracking Eyepiece of the Infrared Stellar Photometer on the Mount Wilson 100-inch Reflector	31
11	The X-Color Index as a Function of Temperature	52
12	The Y-Color Index as a Function of Temperature	53
13	The Observed X-Index Minus the Blackbody Calculated X-Index as a Function of Temperature for Normal Giants .	54
14	The Observed X-Index Minus the Blackbody Calculated X-Index as a Function of Temperature for Supergiants . .	55
15	The Observed Y-Index Minus the Blackbody Calculated Y-Index as a Function of Temperature for Normal Giants .	56
16	The Observed Y-Index Minus the Blackbody Calculated Y-Index as a Function of Temperature for Supergiants . .	57
III-1	Apparent Irradiance of Objects Having Various Magnitudes and Distances	78

REFERENCES

1. EK/ARD ED-442, Semi-Annual Report on a Space Background Study, Eastman Kodak Company, Apparatus and Optical Division, July 8, 1960.
2. EK/ARD ED-575, Semi-Annual Report on a Space Background Study, Eastman Kodak Company, Apparatus and Optical Division, January 16, 1961.
3. EK/ARD ED-692, Semi-Annual Report on a Space Background Study, Eastman Kodak Company, Apparatus and Optical Division, July 17, 1961.
4. Hall, F.F., Proc. IRIS 6, 137 (1961).
5. Hynek, J.A., Editor, "Astrophysics," p. 19-20, McGraw-Hill Co. (1951).
6. Kuiper, G.P., Struve, O., Stromgren, B., Astrophys. J. 86, 571 (1937).
7. Wilson, R.E., General Catalogue of Stellar Radial Velocities, Carnegie Institution, Mount Wilson Observatory (1953).
8. Gates, D.M. J., Opt. Soc. Am. 50, 1299 (1960).

I. INTRODUCTION

The Eastman Kodak Company and its subcontractor, the Ohio State University Research Foundation, have been given the assignment to investigate and characterize the space background problem as faced by optical space defense systems, with primary emphasis on the infrared spectral region. This research is a part of Project Defender, sponsored by the Advanced Research Projects Agency, and directed by the Army Rocket and Guided Missile Agency.

The importance of the role of optical sensors in the development of systems for space defense, surveillance, attitude control and navigation is generally recognized. One of the major problems associated with the development of these systems is that of discrimination, due to the great number of optically detectable objects in a typical space background. Detailed information on the space background in the infrared region has been lacking to the designer of optical systems for space application, and the research pursued under this contract has been directed to meet this urgent requirement.

The first phase of the space background study was devoted to an intensive literature search, and to the development of a theoretical model of the infrared stellar background (reference 1). This model is based on computations which assume that the stars radiate as blackbodies over

their entire range of spectral emittance. A summary table presenting the theoretical infrared magnitudes of 235 light stars is included in this report. See Appendix IV.

The second phase of the study has been designed to test the foregoing theoretical assumptions by implementing a program of observation and measurement of stellar infrared irradiances. The instrumentation of this project was developed, designed and constructed by the Apparatus and Optical Division of the Eastman Kodak Company and is described in detail in references 2 and 3. This instrumentation is designed for use with existing large telescopes and has been employed on the 69-inch reflector of the Perkins Observatory, Delaware, Ohio, and the 60 and 100-inch reflectors of the Mount Wilson Observatory, Mount Wilson, California. The responsibility of conducting the program of observation and measurement has rested primarily on the astronomers of the Ohio State University Research Foundation. The results of this program to September, 1961, with emphasis on data recently obtained at the Mount Wilson Observatories, is the primary subject of this report.

Personnel directly concerned with this research at the Eastman Kodak Company are: Dr. William H. Haynie, former project engineer and now consultant to the project; Charles F. Gramm, present project engineer; Anthony J.G. Prasil, development engineer. For the Ohio State University Research Foundation, Dr. Walter E. Mitchell Jr. is the supervising astronomer with Mr. Philip E. Barnhart, associate astronomer.

II. TECHNICAL SUMMARY

The emphasis in this study has been placed on the detection of relatively cool (300°K) purely self-emitting targets against typical space backgrounds. A target of this nature has most of the emitted energy concentrated in the far infrared, the intensity maximum falling in the infrared near a wavelength of 10 microns.

The literature survey performed in the initial phases of the study revealed a surprising lack of infrared astronomical information. To the present time only a few detectors of infrared radiation such as the thermocouple, lead sulfide and Golay cells have been directed to astronomical objects. The brightness of approximately 70 stars has been measured in the lead sulfide region but, beyond a wavelength of about 3 microns, the only sources studied optically have been the sun, moon, Mars and Venus.

Lacking infrared astronomical data, the assumption has been made that the stars behave as classical blackbody emitters, and calculations have been made of the color indices and infrared magnitudes of 235 of the brighter stars. This represents an extrapolation into the far infrared employing stellar photosphere temperatures which were deduced from spectra of visible and near visible wavelengths. The extrapolation has produced very striking results in that the total number of interfering stars limited by given target characteristics is only on the order of several hundred when the detecting system is confined to the infrared region beyond 7.5 microns.

A measurement program designed to test the results of the theoretical study has been underway since October, 1960. This program has been implemented with two infrared stellar photometers engineered and constructed by the Eastman Kodak Company for use on the Perkins and Mount Wilson reflecting telescopes. The performance of these equipments has proven, on the whole, highly gratifying and satisfactory considering the advanced and unexplored nature of the work. The latest photometer system is capable of detecting infrared irradiance at the aperture of the 69-inch Perkins reflecting telescope on the order of 10^{-18} watts/cm².

During the observing period, to September 1961, many hundreds of measurements have been made in the infrared of some 77 selected stars. The telescopes employed during this period ranged from the Perkins Observatory 69-inch reflector to the 60 and 100-inch reflectors of the Mount Wilson Observatories.

An analysis of the data obtained to date indicates that certain types of stars such as the supergiants and the latest spectral classes possess an excess of infrared emission in the wavelength bands observed. On the basis of the supergiants alone more than 5 times the number of stars of this type would be detectable than that predicted from blackbody extrapolations. Fortunately, there are relatively few of these stars in a given volume of space. Cool giant stars present a more serious problem because of their excess infrared emission and considerably greater population. Much more study of a fundamental nature is indicated in this area

because there is reason to believe, for example, that corrections to the assumed temperature scale for these cool stars may be justified.

A number of abnormal objects have been observed such as ϵ Aurigae, α Aquarii, and T Corona Borealis. Data obtained from infrared photometry of these anomalous objects have proven both useful and interesting to the astrophysicists and continuing study is in order. There is a real possibility that the first "truly infrared" star has been observed in the case of the ϵ Aurigae companion.

A theoretical study of the infrared characteristics of contracting protostars and dark globules of interstellar matter is presented in Appendix III of this report. It is concluded therein that it may just be possible to detect protostars of the individual type in nearby young clusters using a telescope of large aperture. This assumes a system detectivity of 10^{-17} watts/cm², a conservative value in relation to the measured performance of the photometric equipments.

III. TECHNICAL APPROACH

The initial phase of the space background study, devoted to the collection and presentation of existing infrared astronomical data, revealed that little information was available. Lacking observational data, attention was turned to an investigation of astronomical magnitude systems in order to devise an appropriate system for the intermediate and far infrared. Because atmospheric effects limit ground based observations in the infrared to so-called atmospheric "windows", infrared magnitudes were computed for selected known stars with wavelength limits of 2.0 to 2.4 microns (X-band), 3.2 to 4.2 microns (Y-band), and 7.5 to 13.5 microns (Z-band).

The method of attack has been to assume that stars radiate as blackbodies over their entire range of spectral emission. This assumption leads to the prediction of a "color index" for every star whose temperature is known. This color index is a measure of the difference in irradiance in two wavelength bands within the stellar spectrum. If one of these bands is in the visible, for which data is available on a great number of stars, it is then possible to establish each star on a magnitude scale for the infrared wavelength band in question. Knowing the limiting magnitude observable with a given infrared sensor, it then becomes possible to predict the number of stars of a given spectral type (temperature) which will constitute the space background interference. It is also possible

to predict where these interfering stars will be in the sky, providing stars are restricted to those whose temperatures do not fall below known spectral classifications. A detailed discussion of magnitude systems, color indices, and spectral classifications may be found in reference 2.

A summary list of 235 stars calculated to have the brightest predicted infrared magnitudes has been reproduced in this report and is being used presently as an observing list to test the assumption that the stars emit as blackbodies.

The second phase of the space background study, a program of infrared stellar photometry, was carried out under an extension of the original contract. Engineers of the Eastman Kodak Company have designed and constructed two infrared photometers, using the best available cooled photo-conductive detectors and electronic techniques, for use with large astronomical telescopes. They are small field instruments designed to measure the irradiance of individual stellar objects in three spectral wavebands: 2.0 to 2.4 microns, 3.2 to 4.2 microns and 7.5 to 13.5 microns. These wavebands have been isolated by the use of sharp spectral cut, multi-layer interference filters. The early experimental photometer was installed on the 69-inch reflector of the Perkins Observatory during the fall of 1960. Experience gained in the operation of this instrument proved invaluable in the design of a more elaborate instrument completed for use at Mount Wilson over two observing periods in the summer of 1961.

The results of the recent measurements made at Mount Wilson are detailed in this report and include a comparison of the observed color indices of the stars selected for observation with the predicted color index as a function of stellar surface temperature. A brief discussion of possible sources at temperatures below the presently calibrated stellar temperatures is included under a discussion of the results.

There is reason to believe that there are stars which depart strongly from blackbody emission. Among these are the long period variable stars which show very strong molecular blanketing and variable opacity in the visible region of the spectrum. Also evidence is available that some bodies in the universe have temperatures so low as to eliminate them from the normal classification of temperature because of their extremely low photographic brightnesses. Typical of this kind of object is the supposed infrared companion of ϵ Aurigae.

The possible existence of normal stars at very early stages in their evolution may provide a component to the space background hitherto unobserved in the infrared. A number of known peculiar objects have been included on the observing program to try to assess other possible additions to the background problem.

The data obtained in the summer program at Mount Wilson is presented as well as some possible interpretations and recommendations based upon the experiences obtained in gathering these data.

A theoretical study has been made of the infrared characteristics of protostars and dark globules, including an evaluation of the possibility of observing objects of this nature with present day infrared sensors. This study is presented in Appendix III.

IV. INSTRUMENTATION

In making the first measurements with the 69-inch telescope at the Perkins Observatory, an experimental infrared photometer was used which was designed, developed, and constructed by the Eastman Kodak Company, Apparatus and Optical Division. After the initial series of stellar measurements was obtained, the instrument was modified, and a substantial increase in sensitivity was realized. A description of the experimental photometer and the subsequent revision may be found in references 1 and 2, respectively. The experience gained in operating the revised photometer indicated the direction to be taken in evolving a more sophisticated system, capable of greater sensitivity and precision.

The improved photometer system, also designed and constructed by the Eastman Kodak Company, was put into use at the Mount Wilson Observatory in July, 1961. It basically resembles the experimental photometer but embodies those features which experience and analysis of system parameters indicated would be desirable. The considerations leading to the design of this improved photometer are discussed at length in reference 2. They include the effect of atmospheric on the infrared stellar image, the selection of photoconductive detectors, and methods of obtaining background-limited detector operation. A complete description of the detailed design may be found in reference 3.

A. OPTICAL SYSTEM

The arrangement of the photometer head is shown in Figure 1. Stellar radiation enters from the telescope tailpiece (1) or from the side at (1A) and is reflected alternately by the chopping mirror (6) and the stationary mirror (5) known as the "background mirror", to the visible-infrared dichroic (8) (see also Figure 2). The visible light is transmitted through the dichroic to a diagonal mirror and then to the tracking eyepiece, Figure 1 (9) for visual observation and guidance purposes. The infrared radiation is reflected from the dichroic to an off-axis ellipsoid (10) which reimages the stellar image onto nitrogen-cooled plumbide and helium-cooled Cu:Ge photoconductive detectors after splitting into the proper wavelength bands at the NIR-FIR dichroic (11). The radiation, before reaching the cooled plumbide detector, passes through multi-layer interference filters which define the "X" and "Y" spectral regions. The effective "X" channel spectral response is from 2.0 to 2.4 microns as illustrated in Figure 3, while the "Y" channel is effective from 3.2 to 4.5 microns as shown in Figure 4. The word "effective" is used because the curves in the figures are the products of filter transmittance and normalized detector spectral response. Alternatively, the reference blackbody can be imaged on the detectors via the same optical train by interposing a diagonal mirror, Figure 1 (4).

The method devised to effect a modulation of the stellar radiation is characterized by a very high degree of background discrimination. By

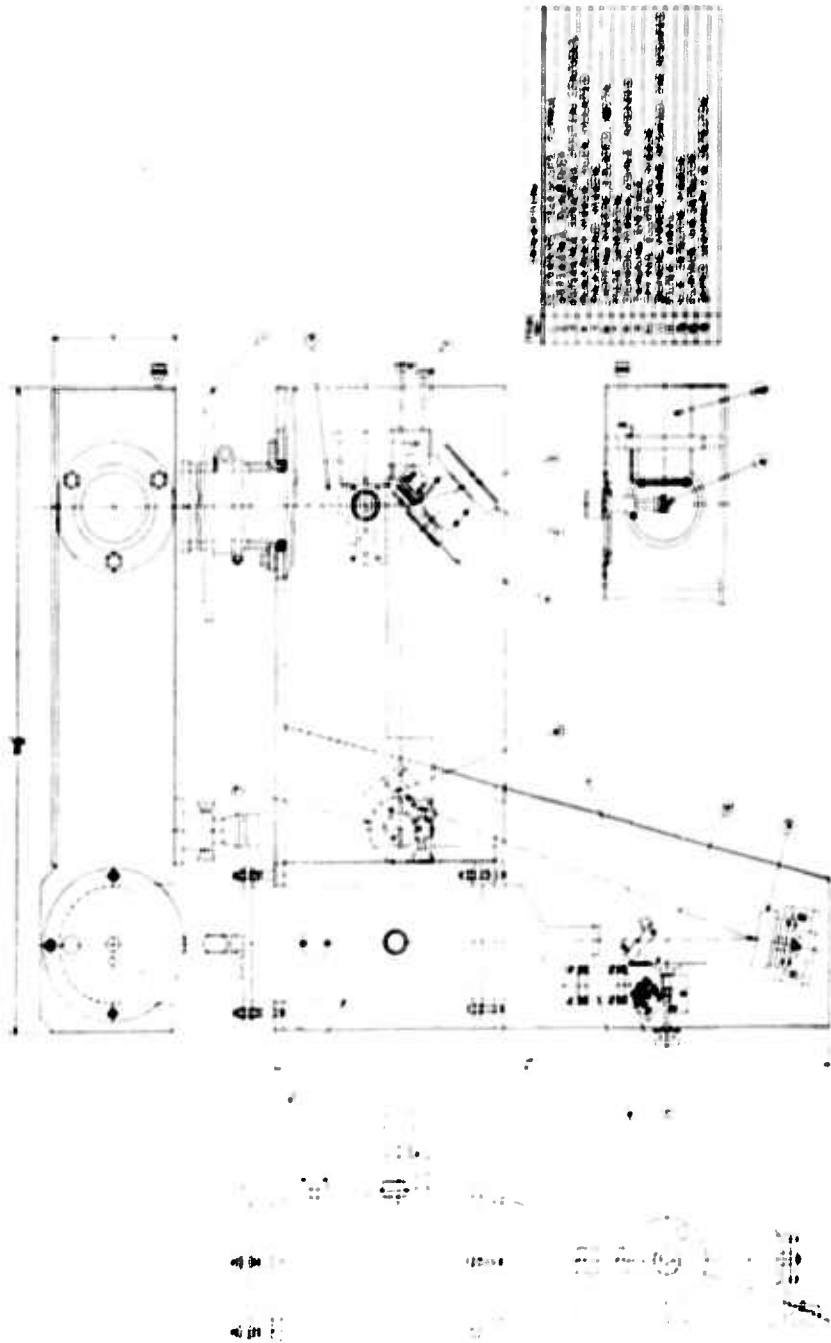


Figure 1. INFRARED STELLAR PHOTOMETER

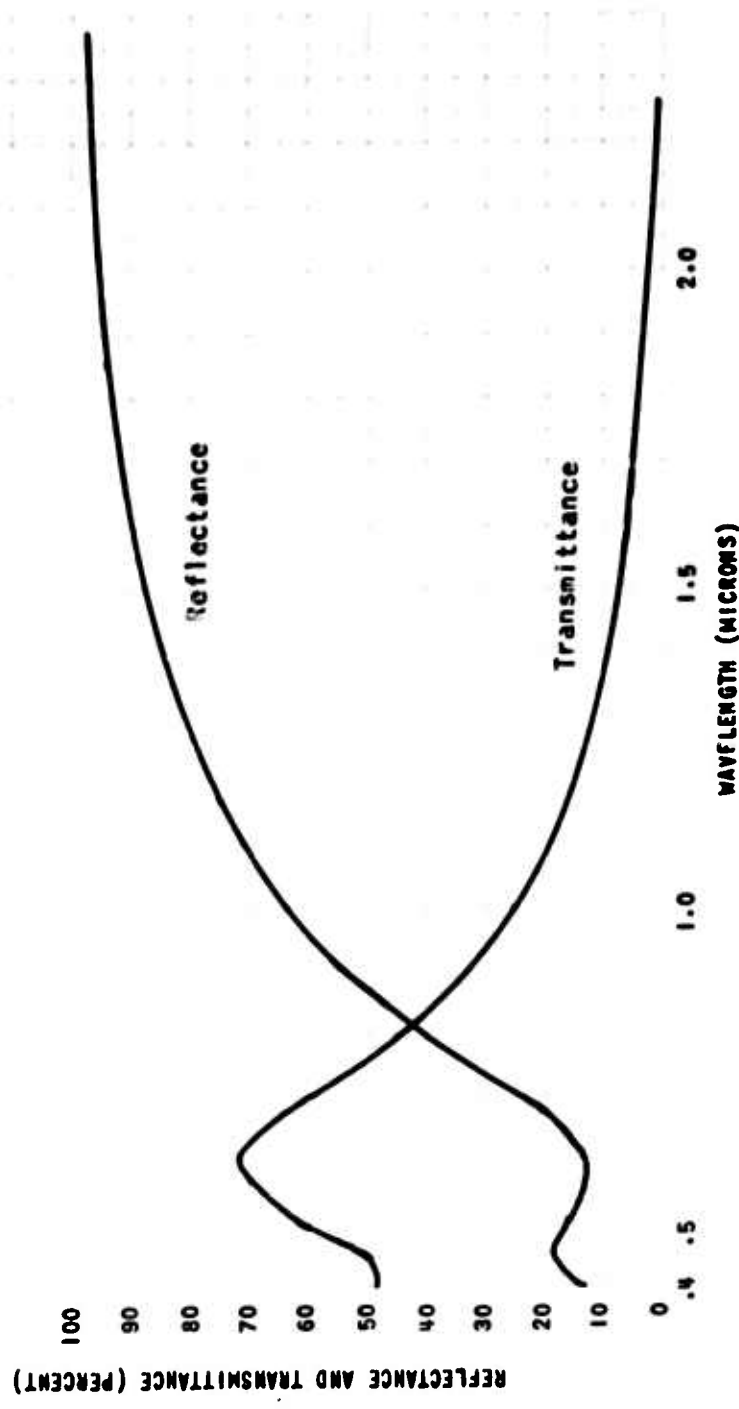


Figure 2. SPECTRAL CHARACTERISTICS OF THE VISIBLE - INFRARED DICHOIC MIRROR

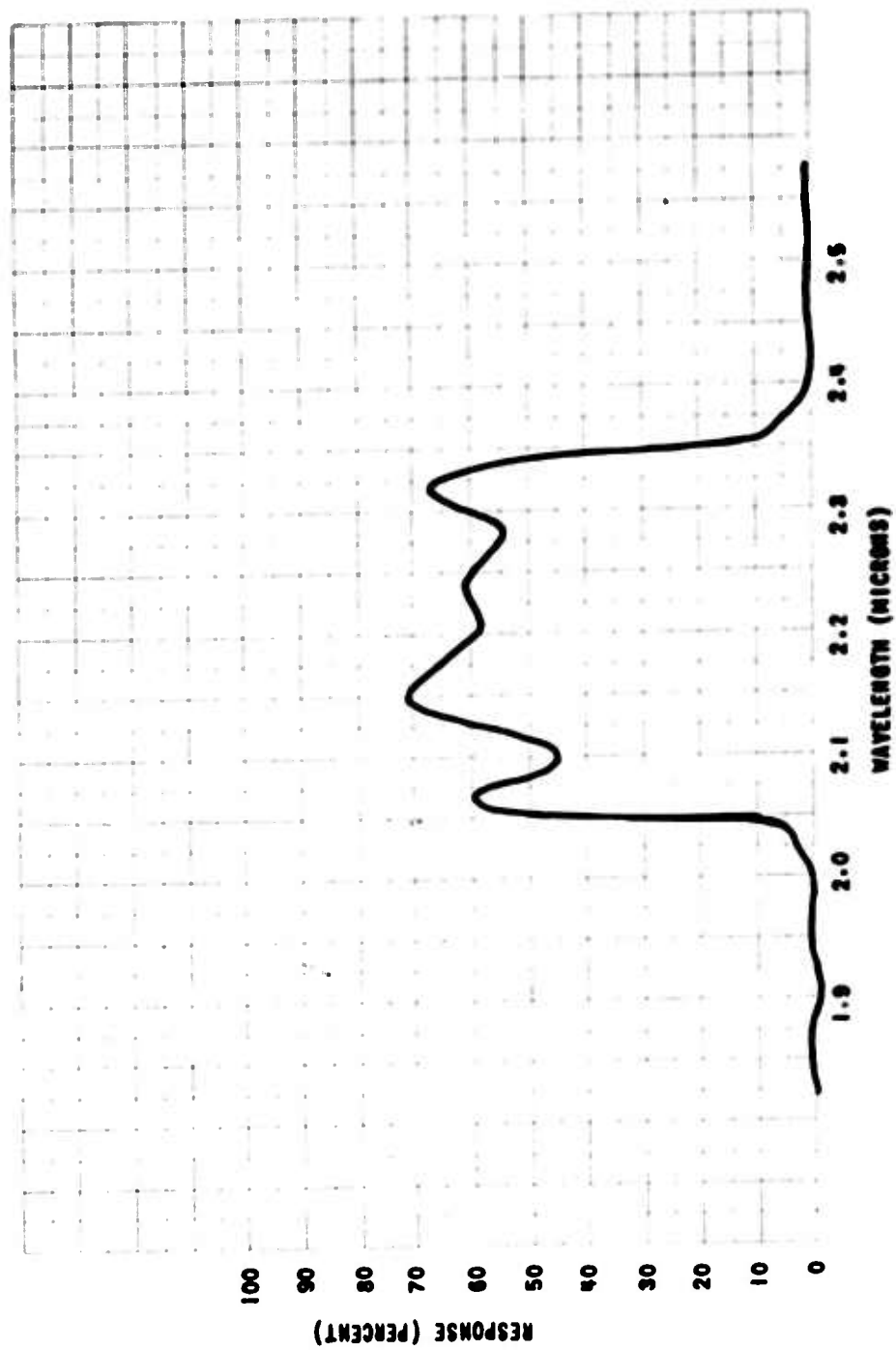


Figure 3. SPECTRAL RESPONSE OF X CHANNEL

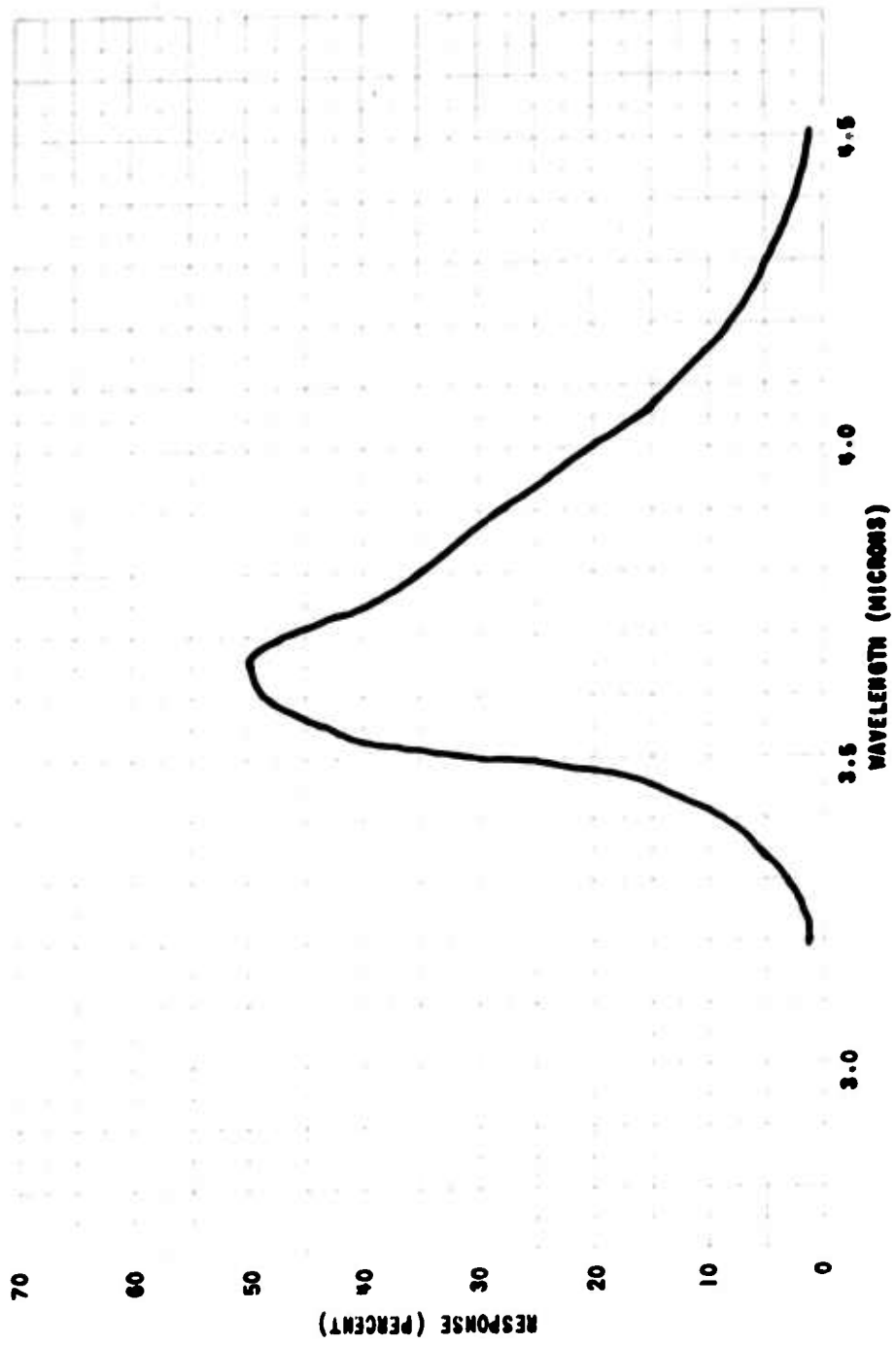


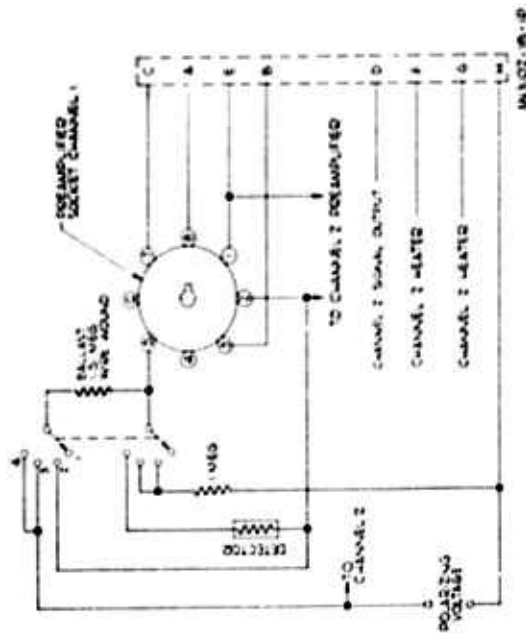
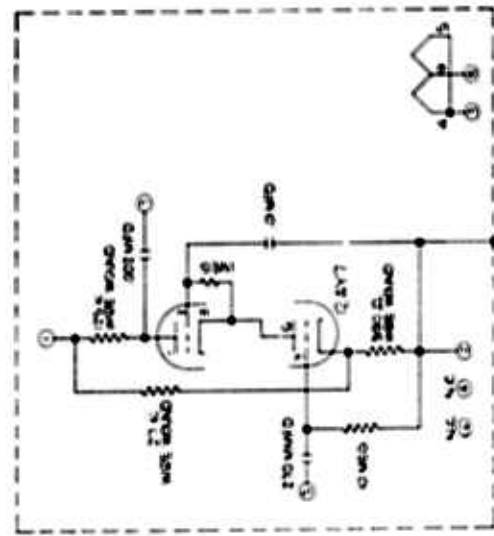
Figure 4. SPECTRAL RESPONSE OF Y CHANNEL

reflecting the radiation alternatively from the rotating chopper mirror and the stationary mirror, the detectors look alternately at the star with surrounding sky background, or only the sky background adjacent to the star. This produces a periodic interruption of the stellar radiation while radiation from the background remains essentially unmodulated.

B. ELECTRONIC SYSTEM

The electronic system makes use of an ac signal preamplifier and amplifier, a synchronous demodulator, a reference signal generator, an integrator with timer, and a recorder. This combination of chopper modulator and synchronous demodulator is sometimes called a homodyne amplifier. This system has the advantage that the electromechanical chopper demodulator does not produce a steady-state dc component when noise only is present, as would a diode demodulator. This allows signal integration to be performed to bring weak signals up out of the noise. Integration times of 10 to 15 minutes may be required for very weak signals. Automatically timed integration periods of one and five minutes are provided. Manual operation is provided to obtain other integration times.

A schematic of the preamplifier is presented in Figure 5. It is of plug-in module form and is located, for minimum noise, in the photometer optical head along with the polarizing battery and detector ballast resistor and switching circuit. The signal amplifier, following the preamplifier, is shown in Figure 6 with the reference generator.



SWITCH POSITION
 1- INPUT SHORTED
 2- INPUT OPEN
 3- POSITIVE BATTERY TEST
 4- OPERATE

NOTES:
 1- SCHEMATIC SHOWS ONLY CHANNEL 1. CHANNEL 2 IS IDENTICAL AND IS ALSO ON THE SAME CHASSIS.

Figure 5. PREAMPLIFIER SCHEMATIC

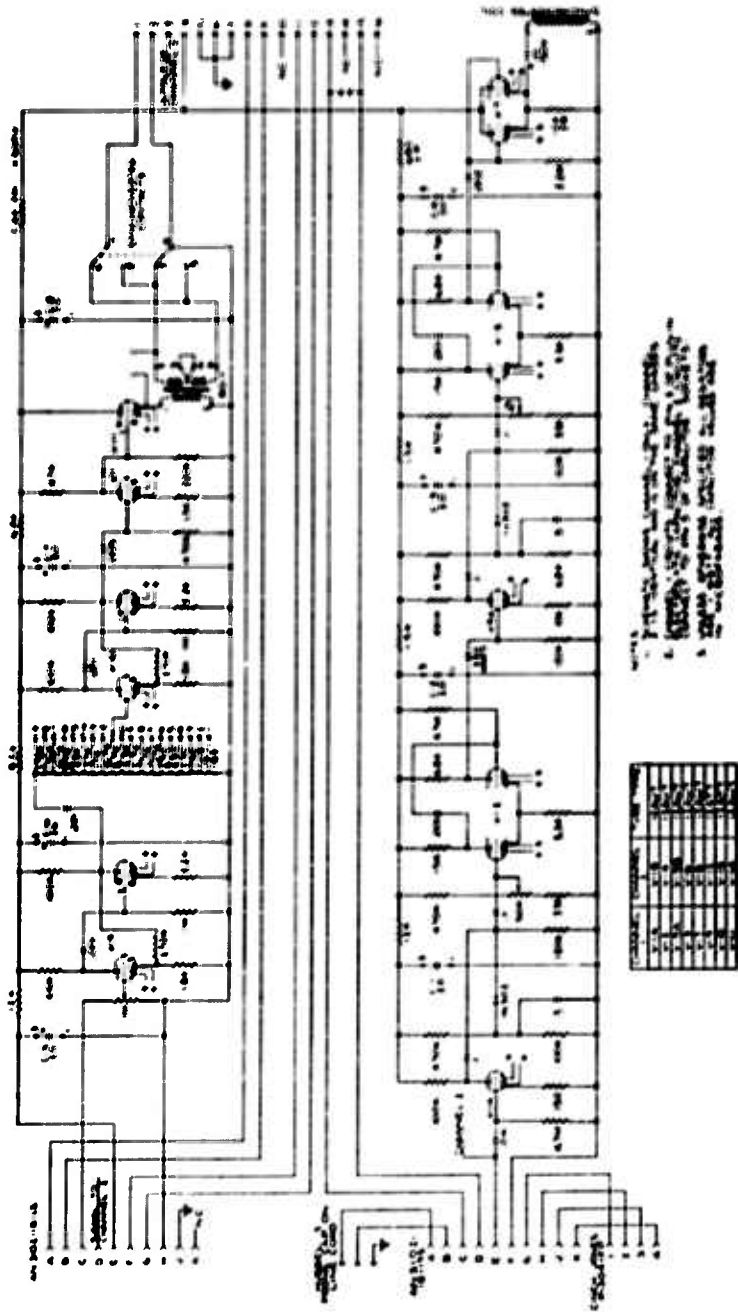


Figure 6. SIGNAL AMPLIFIER AND REFERENCE GENERATOR SCHEMATIC

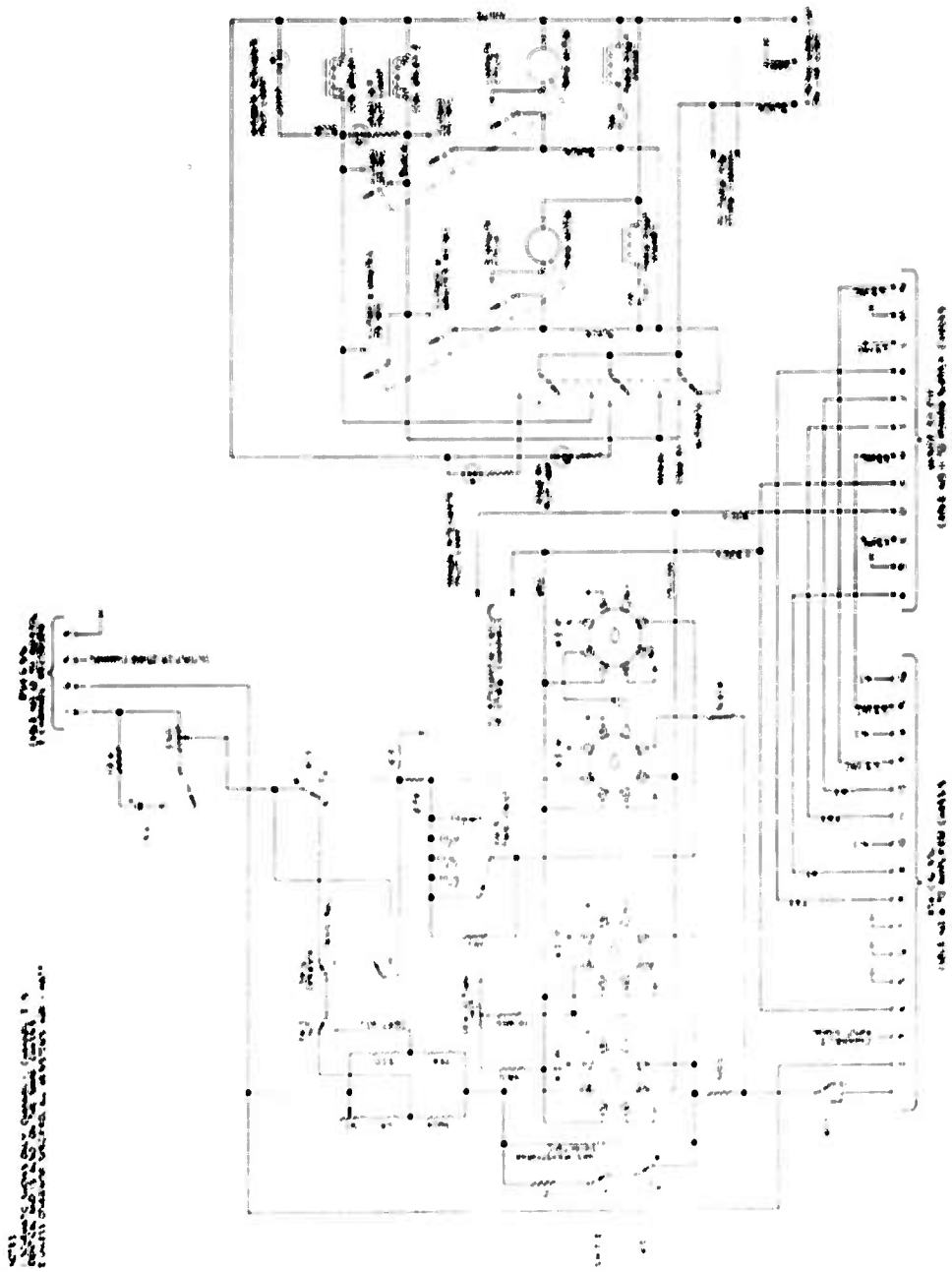


Figure 7. INTEGRATOR AND TIMER SCHEMATIC

Integration is performed by Philbrick plug-in modules. The circuitry used in conjunction with these is given in Figure 7.

C. PERFORMANCE

The second photometer system provides a considerable improvement in detectivity over the previous experimental photometer as well as in extended spectral response to longer wavelengths. The experimental photometer had a minimum electronic bandwidth of 0.2 cycles/sec and, for the 69-inch Perkins reflector, a theoretical NEPD of 10^{-17} watts/cm² for infrared wavelengths to 4 microns. The observed stellar signals were as small as 5×10^{-17} watts/cm². The new photometer, with the 69-inch Perkins reflector, has a theoretical NEPD approaching 7×10^{-19} watts/cm² in the 3 to 4 micron band or an improvement factor in detectivity of about fourteen. This presumes the use of a twenty minute integration interval and effective bandwidth of about 0.001 cycle/sec. The stellar irradiances measured with this photometer at Mount Wilson do not represent the observational threshold of the equipment.

A view of the photometer system set up in its operating position on the 60-inch telescope is shown in Figure 8. The instrument as it was subsequently set up for use in conjunction with the 100-inch Hooker reflector at Mount Wilson is shown in Figures 9 and 10.

As can be inferred from the photographs, operation with the 60-inch telescope was very convenient, since the observer could stand on the floor while looking through the guiding eyepiece. When working in

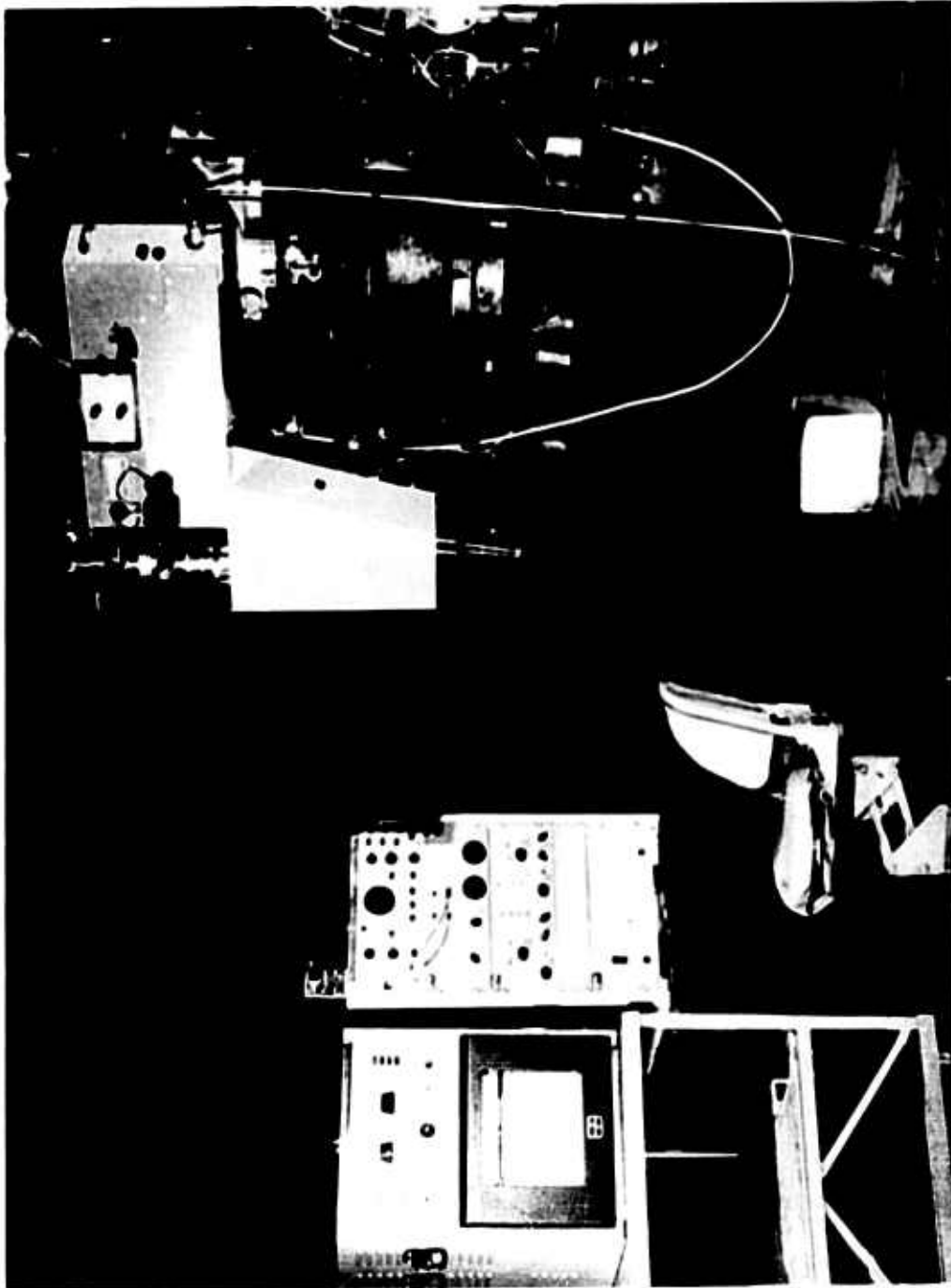


**Figure 8. THE INFRARED STELLAR PHOTOMETER SYSTEM ON THE MOUNT WILSON
60 - INCH REFLECTOR**

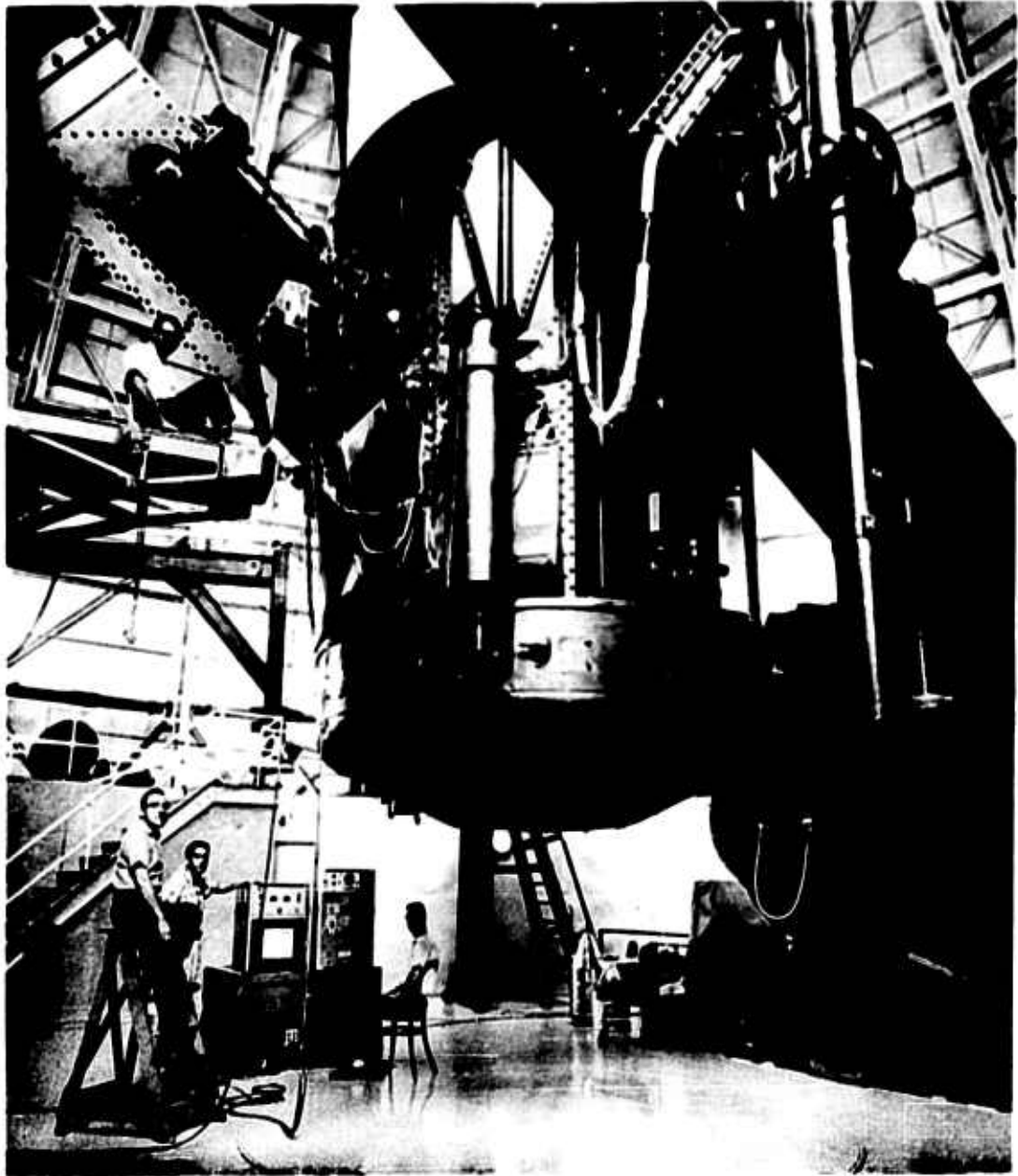
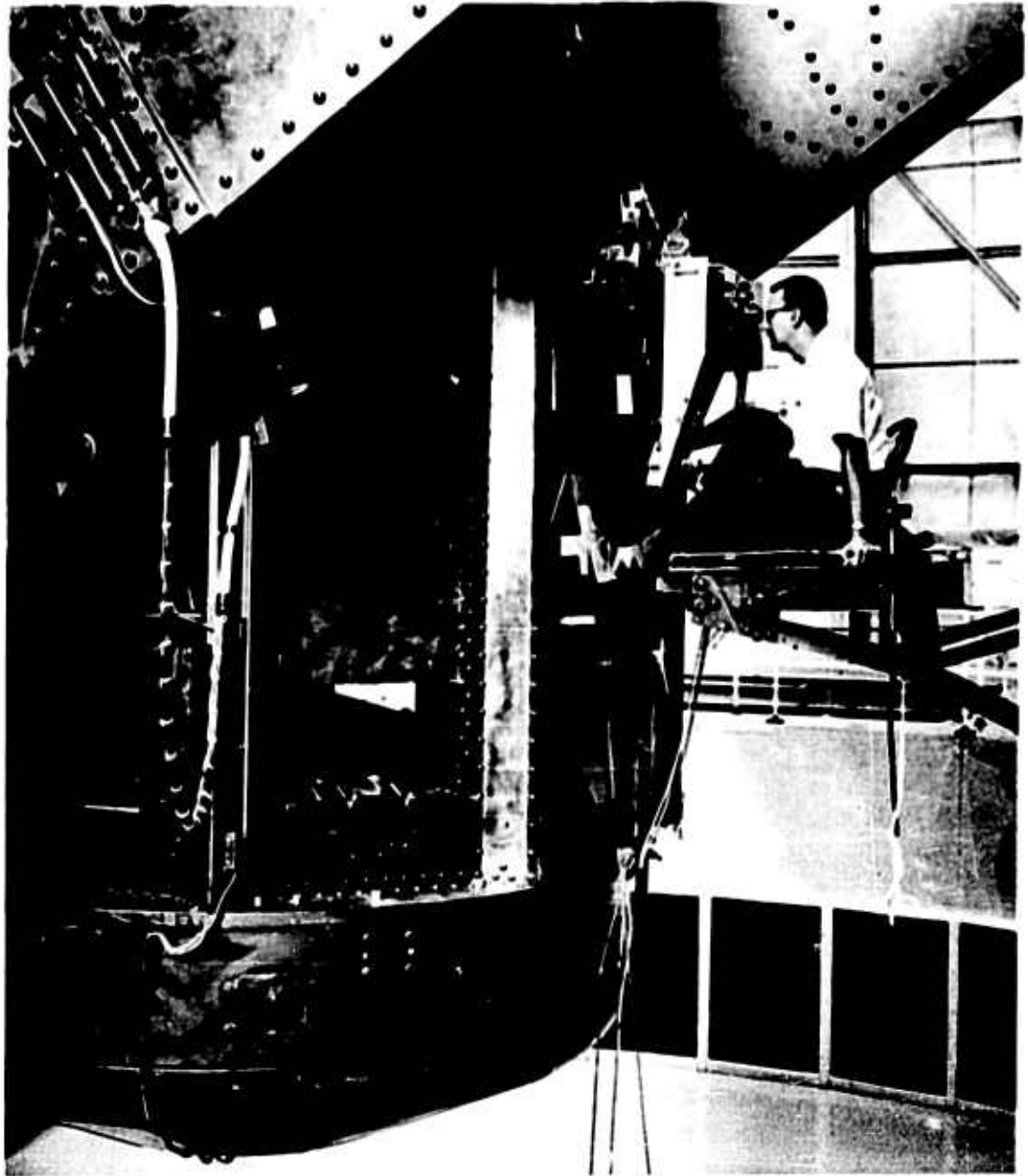


Figure 9. OVERALL VIEW OF THE INFRARED STELLAR PHOTOMETER SYSTEM ON THE MOUNT WILSON 100 - INCH REFLECTOR



**Figure 10. OBSERVER AT THE VISUAL TRACKING EYEPIECE OF THE
INFRARED STELLAR PHOTOMETER ON THE MOUNT WILSON
100 - INCH REFLECTOR**

conjunction with the 100-inch telescope, however, the observer is located on a small platform some 10 feet above the floor. As a result, loading of the liquid helium-cooled dewar is rather difficult for it requires two people to remove and replace it, if it is to be remotely filled. As an alternative, filling the dewar while mounted in the instrument not only requires the services of two people but also requires storage dewars of liquid nitrogen and helium, a gaseous helium supply, and a transfer tube.

V. THE OBSERVING PROGRAM

The observing program was begun in the summer of 1960, soon after the completion of the calculations of the theoretical color indices for the infrared bands. An experimental photometer was designed and built by the Eastman Kodak Company for the purpose of making infrared measurements and determining the feasibility of a more sophisticated instrument. In the course of use of the experimental instrument numerous problems of technique were solved and some deficiencies of design overcome.

Observations were obtained on eleven nights between July 9, 1960 and December 12, 1960, using the experimental photometer on the 69-inch telescope at the Perkins Observatory. The majority of these observations were made in the 2.0 to 2.4 micron region. The early detectors were not sensitive enough in the 3 to 4 micron band to produce usable signals. The now familiar problems of sine-wave interference arising from objects adjacent to or included in the cone of view of the detector were encountered in the Y-band to such an extent that the telescope and photometer were themselves producing signals far in excess of what we were trying to observe from the stars. As these problems were corrected more and more effort was devoted to the longer of the two wavelength bands toward the end of the 1960 observing season.

From the middle of December 1960 to the middle of March 1961 the weather was uniformly poor and no opportunity to obtain further data with the experimental photometer presented itself. Unfortunately when the weather did begin to clear toward the end of March the dismantling of the 69-inch telescope in preparation for its relocation in Flagstaff, Arizona, had already begun and it was not possible to use the instrument for measurements.

The period during which the 69-inch telescope was shut down marked the time when work was started on the design for a new, two-channel, stellar infrared photometer by the engineers at Eastman Kodak Company. This instrument was completed in July 1961 and delivered just after the start of the observing period on Mount Wilson. When it became apparent there would be no telescope time available at the Perkins Observatory before the termination of the contract period, an observing period at Mount Wilson was generously arranged by the director of the Mount Wilson and Palomar Observatories.

The 60-inch run provided an opportunity to get the new photometer operating and give the observers experience before going to the 100-inch telescope.

During the observing period on Mount Wilson, observations were made on 52 stars in both shorter wavelength bands. There had been 33 stars observed at the Perkins Observatory in the last six months of 1960, some of which were re-observed at the Mount Wilson Observatory. Of the 33 stars observed in Ohio, 14 were observed in both the X- and Y-bands and of these only

8 were observed, also in both bands, at Mount Wilson. Thus the Mount Wilson trip increased by 44 the number of stars observed in both wavelength bands.

Since the procedures involved in the observing and reduction of the data obtained at both locations are the same, a separate discussion of the two sets of data will not be included in this report. A complete discussion of the 1960 observations is included in Reference 2 and the only reference to these data will be in connection with a comparison of the data obtained at Mount Wilson. A summary table of the stellar measurements made at the Perkins Observatory has been reproduced in Appendix V.

A. GATHERING OF DATA AND OBSERVING CONDITIONS ON MOUNT WILSON

The Ohio State - Eastman Kodak observing team was assigned 8 nights in July on the 60-inch reflector for the purpose of testing equipment and making whatever observations might be possible. As the new photometer had not arrived at the mountain at the start of the run (July 18) the experimental photometer was attached to the telescope and observations were begun with this instrument. Considerable alignment difficulty was encountered on the telescope and during the first night on the telescope much time was spent in achieving optical alignment satisfactory for observing. The following afternoon was used to obtain a careful internal alignment of the instrument. Soon after the photometer was replaced on the telescope it was necessary to shut down operations due to high winds. When the wind in the mountains of southern California exceeds about 25 knots considerable quantities of dust

and ash resulting from forest fires is carried aloft and scattered about the countryside. If the dust content of the air becomes too large it is desirable to close down the telescopes to protect the optical surfaces. The observations were cut short the second night and as the wind remained high throughout the following day it was decided not to open the dome at all the third night.

Just before the time to begin work on the third night the new photometer arrived on the mountain. The night was spent in unpacking and assembling the new equipment on the telescope. The experimental photometer was put aside as a standby instrument throughout the rest of the Mount Wilson observing period.

During the final assembly of the new photometer at the telescope, an unfortunate accident occurred. The visual-infrared dichroic beamsplitter was mounted in reverse in the bracket provided for it and the result was a loss of nearly 4 magnitudes in the Y-band due to the absorption in the glass of wavelengths longer than about 2.7 microns. As the glass is nearly transparent to the wavelengths shorter than 2.7 microns, the observations in the X-band came through with the anticipated strength. This occurrence resulted in a considerable loss of telescope time with the result that the observing period was in the nature of a practice run. It was not

until the photometer was bench-tested between the 60-inch and 100-inch runs that the reversal of the dichroic was discovered.

The weather in southern California is usually well suited for astronomical observations, and the month of August is usually among the best months in that part of the United States. It was felt, therefore, that when the project was assigned 10 nights on the 100-inch telescope virtually all of these nights would prove useful. As a matter of fact the official record book kept for the 100-inch telescope shows that during the past 20 years only one month of August has had more than 5 nights in the entire month which could not be used for observation because of cloudy weather. Up to the time that the Ohio State University - Eastman Kodak run came to an end on August 23 there had been 8 nights closed out by the weather and 5 of these had come during the 10 nights scheduled to the project. Despite the curtailed observing time, many observations were obtained on the good nights.

In addition to the many nighttime hours spent by the members of the observing team during the telescope runs, much time was devoted during the afternoons to trying to place the liquid helium dewar in operating condition for the attempts at observing in the 8 to 14 micron region. The main difficulty was obtaining and holding an adequate vacuum in the outer jacket of the dewar. It was not until the ninth night of the 100-inch run that the first successful transfer of helium was made. Dr. A. Hildebrand of the Jet Propulsion Laboratory very generously provided a transfer tube of his own

construction and the initial transfer was carried out under his personal direction. The loaded dewar was placed on the telescope on two nights, both of which were intermittently cloudy, and no positive results were obtained. There was considerable difficulty in attaining sufficient alignment of the longwave detector along with the shortwave detector in order to use the instrument in the way in which it was intended, namely, that the shortwave detector signal be used for guiding by the observer while the signal from the longwave detector is being integrated.

There was a hopeful sign noted in connection with the operation of the helium dewar. The supply of helium in the dewar from a single filling lasted for a total of about 20 hours without being topped off during the interim. The nitrogen jacket was filled twice during the period. This seems to indicate the feasibility of filling the 1.2-liter dewar at a cryostat and transporting it to the telescope rather than attempting to transport and store a 10- or 15-liter supply of helium near the telescope.

B. ANALYSIS OF THE DATA

In the Mount Wilson program it was decided to obtain as many observations of different stars as possible. It was felt that this would provide a more complete survey (though still provisional from the point of view of precision) of the nature of these objects in the infrared.

A brief description of the techniques of data reduction used on this program is given in Appendix I. The results of the reduction are listed in Table I* and a catalogue of the observed magnitudes and color indices for the program stars is given in Table II.* A comparison of the results obtained at Mount Wilson with those obtained at Perkins Observatory for the stars observed at both locations in both the X- and Y-bands is given in Table III.*

C. ATMOSPHERIC EXTINCTION

The earth's atmosphere absorbs radiation to a greater or lesser extent over the entire wavelength range of the electromagnetic spectrum. In the visible region of the spectrum this absorption and scattering may amount to a few tenths of a stellar magnitude at the zenith and much more at directions far from the zenith where the light must traverse a long path throughout the atmosphere. The exact amount of obscuration in a given wavelength band depends upon the amount and relative effectiveness of the atmospheric components contributing to the absorption. In the course of astronomical photometry the extinction measurements ordinarily are taken systematically along with the observations of the stars in question.

The minimization of extinction effects in the Mount Wilson program suggested that the observations of each star be made near to the meridian, insuring that the star be as near the zenith as possible and its light thereby subject to a minimum of atmospheric absorption. In practice some of the program stars could not be observed on or very near to the

* Tables I, II and III follow page 41.

meridian. Some of them were located so far south that even though they were observed on the meridian they were at very large zenith distances. Definitive corrections for atmospheric extinction are not applied to the data in this report.

However, from Reference 3, page 54, and Reference 8, page 1304, one can estimate the size of the magnitude corrections to zenith (i.e., to unit air mass) resulting (primarily) from continuous atmospheric absorption by water vapor: $-0.3(\sec z - 1)$, where z is the zenith distance. This correction is negligible (i.e., less than 0.1) for all but 6 observations (stars Nos. 22, 136, 148, 224, 229) and exceeds -0.14 for only one observation (star No. 155). Correction of the measured x and y magnitudes to zero air mass is implicit in the adoption of $m_x = m_v$ and $m_y = m_v$ for a star at a temperature of 11000°.

One attempt was made to determine the extinction characteristics of one night, but the results were complicated by another quite unforeseen occurrence. The detectors which were used demonstrated a rather large fluctuation in sensitivity with time. In spite of the fact that the data intended for use as extinction measures were lost, due to the unstable sensitivity, there is some indirect indication that there may be serious extinction effects in the infrared. Some of the bright infrared objects which were observed at consistently large zenith distances displayed the greatest dispersion in measured values. These objects, because of their greater

brightness, should be observed with the greater precision. An account for this discrepancy may be given on the assumption that these stars are indeed the ones most readily affected by the variations in atmospheric extinction from night to night. To test this assumption is the first task assigned to the observing program when the stellar infrared photometer is again installed on a telescope.

D. DAYTIME OBSERVING

On August 21, 1961, observations were made on α Tau continuing into the dawn, as planned in the observing schedule outlined in Reference 3, page 55. The telescope was lined up on the star before dawn and X and Y channel readings were taken. α Tau, which is number 37 on our list, has a visual magnitude of 1.1, $m_x = 2.5$, and $m_y = 2.8$. Readings were continued as the sky brightened and until it and the other first magnitude stars were no longer visible. The deflections obtained were constant over the entire observing period. More work is required in this direction to determine the daytime limit of the photometer. Only one star can be observed into each dawn as it is probably impossible, with the small field of view of the photometer, to find a star when it is not visible in the sighting telescope eyepiece.

E. DISCUSSION OF THE RESULTS

The observed apparent magnitudes in the X- and Y-bands of all the stars measured at Mount Wilson are included in Table I. The table consists of the following information: the star designation, including the IR

TABLE I A
MOUNT WILSON SUMMARY DATA SHEET FOR X-RAY

STAR	OBSERVED m_x					Computed m_x
	8/14-15	8/15-16	8/16-17	8/17-18	8/19-20	
6 TV Pic		+0.1	-0.3			-0.2
8 δ And	+0.6		+0.2::	+0.5		+0.3
9 α Cas			-0.4::			+0.2
14 δ And	-1.7	-1.8	-2.2::	-1.7		-1.5
20 γ And	-0.8	-0.8	-1.5::			-1.1
21 α Ari	-0.6		-1.5::			-0.7
22 θ Cet	-2.9	-3.1	-4.0::	-2.9		-4.0
24 η Per		+0.1				+0.4
25 α Cet		-1.6	-2.7::	-1.6		-1.4
26 ρ Per	-1.9	-1.9				-1.9
37 α Tau		-2.7		-3.1		-2.5
41 ϵ Aur				-0.8		-0.5
134 α Boo		-3.6::	-1.4::	-3.4		-2.5
148 α Ser			+1.8::			-0.4
155 α Sco				-3.5		-3.0
156 30 Her			-2.3	-1.9		-1.0
167 α Her		-3.9::	-3.7	-3.5		-2.1
180 χ Oph				-1.5		-0.1
182 R Lyr		-2.4	-2.3	-2.1		-1.6
193 δ Lyr		-1.4		-1.3		-0.6
198 γ Aql				-1.0		-0.7

TABLE I A (Cont'd.)

MOUNT WILSON SUMMARY DATA SHEET FOR X-BAND

STAR	OBSERVED m_x						Computed m_x
	8/14-15	8/15-16	8/16-17	8/17-18	8/19-20	8/20-21	
189 δ Sge			-0.8	-1.0			-0.6
190 \times Cyg			-1.7	-2.1	-2.1		-4.1
192 γ Sge				-0.5			-0.4
198 U Del			-0.7	-0.7			-0.4
199 ϵ Cyg				0.0			-0.1
210 W Cyg			-1.1	-1.6			-0.1
211 ϵ Peg				-0.9			-0.7
212 μ Cep	-1.7	-1.7		-1.9			-0.9
213 18 Cep		0.0					-0.1
216 ζ Cep		+0.2		-0.2			-0.4
224 λ Aqr			-0.3	-0.4			-0.6
225 β Peg	(-2.2)	(-2.2)	-1.9	(-2.2)	(-2.2)	(-2.2)	-1.8
229 \times Aqr				+2.0	+1.6		-0.5
231 71 Peg		-0.2	+0.3 +0.2		+0.3	-0.5	-0.1
234 γ Peg	0.0	+0.1	+0.1 +0.2		-0.1	-0.1	+0.1
235 R Cas	-1.4	-1.2	-1.5	-1.3		-1.1	-1.6
α Lyr		(-0.1)	(-0.1)	(-0.1)			
α Aql							
δ Cep	+2.3			+2.3			
ϵ Aur				+1.3			

TABLE I B
MOUNT WILSON SUMMARY DATA SHEET FOR Y-BAND

STAR	OBSERVED m_y						Computed m_y
	8/14-15	8/15-16	8/16-17	8/17-18	8/19-20	8/20-21	
6 TV Psc		-0.1	+0.3::				-0.6
8 6 And	+0.5	+1.1	+0.6::	+0.4		+0.6	-0.3
9 α Cas			+0.4::				0.0
14 β And	-2.3	-1.9	-1.6::	-2.0		-1.3	-1.9
20 γ And	-1.2	-0.8	-0.8::				-1.4
21 α Ari	-0.8		-0.5::			+0.2::	-1.0
22 σ Oct	-3.7	-3.4	-3.4::	-3.7		-2.2::	-4.4
24 η Per		+0.2				0.0	0.0
25 α Oct		-1.6	-1.7::	-2.0		(-1.7::)	-1.8
26 ρ Per	-2.2 -2.2	-2.0					-2.3
37 α Tau		-2.8		-3.2		-2.7::	-2.8
41 ϵ Aur				-1.1			-0.8
86 α Boo			-1.2::	-3.4			-2.7
148 α Ser							
155 α Sco				-3.9			-3.4
156 30 Her			-1.1::	-2.7			-1.2
167 α Her		-3.5	-3.0	-3.9			-2.4
180 X Oph				-2.2			-0.3
182 R Lyr	-1.3	-2.8	-1.6	-2.4	-1.9 -2.0		-1.9
183 6 Lyr		-2.3		-1.6			-1.0
188 γ Aql				-0.9			-1.0

TABLE I B (Cont'd.)

MOUNT WILSON SUMMARY DATA SHEET FOR Y-BAND

STAR	OBSERVED m_y						Computed m_y
	8/14-15	8/15-16	8/16-17	8/17-18	8/19-20	8/20-21	
189 δ Sco			+0.1	-1.1			-1.0
190 α Cyg			-1.2	-2.9	-2.4		-4.3
192 γ Sco				-0.8			-0.6
198 U Del			-1.1	-1.4			-0.6
199 ϵ Cyg				0.0			-0.3
210 η Cyg			-1.3	-2.1			-0.5
211 ζ Peg				-1.4			-1.0
212 μ Cep	-2.0 -2.0	-2.1 -2.2		-2.5			-1.3
213 18 Cep		-0.1					-0.4
216 ζ Cep		+0.1		+0.3			-0.8
224 λ Aqr			+0.4	-0.5			-1.1
225 β Peg	(-2.3)	(-2.3)	-2.0	(-2.3)	-2.1	(-2.3)	-2.3
229 X Aqr				+2.0	+1.4		-0.8
231 71 Peg		-0.1	+0.1		-0.4	-0.3	-0.4
234 ψ Peg	-0.2	-0.1	+0.2 +0.2		+0.3	+0.2	-0.3
235 R Cas	-2.4 -2.3	-1.9	-1.9	-2.2		-2.0	-1.3
α Lyr		(-0.1)	(-0.1)	(-0.1)	(-0.1)		-0.1
α Aql				-0.9			
δ Cep				+2.9			
ϵ Aur				+1.2			

TABLE II

CATALOGUE OF MOUNT WILSON OBSERVATIONS

Star Designation

IR No.	Name	Sp T	\bar{v}_y	\bar{v}_x	X.I.	H_x (watts/cm ²)	\bar{v}_y	Y.I.	H_y (watts/cm ²)	T_{eff} (°K)	% Obs
6	TV Psc	G M3	+4.6	-0.1	-4.7	2.2×10^{-15}	-0.1	-4.7	3.3×10^{-16}	2980	2.1
8	δ And	G K3	+3.5	+0.6	-2.9	1.1×10^{-15}	-0.7	-2.8	1.6×10^{-16}	3660	3.4
9	π Cas	G G7	+2.5	-0.4	+2.9	2.8×10^{-15}	-0.4	-2.1	2.1×10^{-16}	4500	1.1
14	ε And	G M0	+2.4	-1.8	-4.2	1.0×10^{-14}	-2.0	-4.1	2.0×10^{-15}	3400	4.4
20	γ And	G K3	+2.3	-0.5	-3.1	4.2×10^{-15}	-1.0	-3.3	7.0×10^{-16}	3660	2.2
21	α Ari	G K1	+2.2	-0.6	-2.8	3.5×10^{-15}	-0.8	-3.0	6.1×10^{-16}	4000	3.3
22	ο Cet	G M6e	(+4.4)	-3.0	(-7.4)	3.2×10^{-14}	-3.6	(-8.0)	6.5×10^{-15}	2600	3.3
24	γ Per	G M0	+3.9	+0.1	+3.8	1.8×10^{-15}	-0.2	-3.7	2.5×10^{-16}	3820	1.1
25	γ Cet	G M1	+2.8	-1.6	-4.4	7.2×10^{-15}	-1.8	-4.6	1.6×10^{-15}	3200	2.2
26	ρ Per	G M4	+3.2	-1.9	-5.1	1.2×10^{-14}	-2.1	-5.3	2.2×10^{-15}	2850	2.3
37	γ Tau	G K5	+1.1	-2.9	-4.0	2.9×10^{-14}	-3.0	-4.1	4.9×10^{-15}	3550	2.2
41	δ Aur	G K3	+2.9	-0.8	-3.7	4.2×10^{-15}	-1.1	-4.0	6.1×10^{-16}	3660	1.1
136	α Boo	G M0	+0.2	-3.4	-3.6	4.6×10^{-14}	-3.4	-3.6	7.1×10^{-15}	4200	1.1
148	ε Ser	G M2	+2.8	+1.8	-1.0	3.8×10^{-16}	--	--	---	3950	1.0
155	γ Sco	G M1	+1.2	-3.5	-4.7	5.0×10^{-14}	-3.9	-5.1	1.1×10^{-14}	3100	1.1
156	306 Her	G M5	+5.0	-2.1	+7.1	1.4×10^{-14}	-2.7	-7.7	3.6×10^{-15}	2600	2.1
167	δ Her	G M5	+3.5	-3.6	-7.1	5.6×10^{-14}	-3.5	-7.0	7.7×10^{-15}	2710	1.1
180	δ Oph	G M6e	+5.9	-1.5	+7.4	7.9×10^{-15}	-2.2	-8.1	2.4×10^{-15}	2600	1.2
182	R Lyr	G M5	(+4.7)	-2.3	(+7.9)	1.7×10^{-14}	-2.0	(-6.7)	2.0×10^{-15}	2710	3.6
183	ε Lyr	G M4	+4.5	-1.4	+5.9	7.2×10^{-15}	-1.6	+5.1	1.3×10^{-15}	2850	2.1
188	γ Aql	G K4	+2.8	-1.0	+3.8	5.0×10^{-15}	-0.9	-3.7	7.0×10^{-16}	3600	1.1

TABLE II (Cont'd.)
CATALOGUE OF MOUNT WILSON OBSERVATIONS

Star Designation

IR No.	Name	Sp T	M_V	M_X	X.I.	M_X (watts/cm ²)	M_Y	Y.I.	M_Y (watts/cm ²)	Temp. (°K)	M_{OBS}
189	δ Sge	6 M2	+3.8	-0.9	+4.7	4.6×10^{-15}	-0.5	-4.3	4.8×10^{-16}	3090	2,2
190	χ Cyg	6 M7	(+10.7)	-2.0	(+12.7)	1.3×10^{-14}	-2.3	(+13.0)	2.6×10^{-15}	2690	3,3
192	γ Sge	6 M0	+3.7	-0.5	+4.2	3.2×10^{-15}	-0.8	-4.5	6.4×10^{-16}	3340	1,1
198	U Del	c M6	+5.6m	-0.7	+6.3	3.8×10^{-15}	-1.3	-6.9	1.0×10^{-15}	2550	2,2
199	ε Cyg	6 M0	+2.6	0.0	+2.6	2.0×10^{-15}	0.0	+2.6	3.0×10^{-16}	4200	1,1
210	η Cyg	6 M4e	+5.0m	-1.4	-6.4	7.2×10^{-15}	-1.7	-6.7	1.5×10^{-15}	2690	2,2
211	ε Peg	c M0	+2.5	-0.9	+3.4	4.6×10^{-15}	-1.4	-3.9	1.1×10^{-15}	3620	1,1
212	μ Cep	c M2e	+3.6	-1.8	+5.4	1.0×10^{-14}	-2.2	-5.8	2.4×10^{-15}	3050	3,5
213	18 Cep	6 M5	+5.5	0.0	+5.5	2.0×10^{-15}	-0.1	-5.6	3.3×10^{-16}	2710	1,1
216	ζ Cep	c M5	+3.6	0.0	+3.6	2.0×10^{-15}	+0.2	-3.4	2.5×10^{-16}	3390	2,2
224	γ Aqr	6 M2	+3.8	-0.4	+4.2	2.8×10^{-15}	-0.5	-4.3	4.8×10^{-16}	3090	3,1
225	δ Peg	6 M2	+2.6	-2.2	+4.8	1.6×10^{-14}	-2.3	-4.9	2.6×10^{-15}	3090	7,7
229	χ Aqr	6 M5	+5.1	+1.8	+3.3	3.8×10^{-16}	+1.7	+3.4	6.4×10^{-17}	2710	2,2
231	τ Peg	6 M5	+5.5	-0.1	+5.6	2.2×10^{-15}	-0.2	-5.7	3.7×10^{-16}	2710	5,4
234	ν Peg	6 M3	+4.8	0.0	+4.8	2.0×10^{-15}	+0.1	-4.7	2.8×10^{-16}	2930	6,6
235	R Cas	6 M7e	(+10.9)	-1.3	(+13.0)	6.5×10^{-15}	-2.1	(+13.0)	2.2×10^{-15}	2590	5,6
D	α Lyr	A2	+0.1	-0.1	+0.2	2.2×10^{-15}	-0.1	-0.2	3.3×10^{-16}	9700	2,3
E	δ Aql	A2	+0.9	--	--	---	-0.9	-1.8	7.0×10^{-16}	10300	0,1
H	δ Cep	G0	+3.7	+2.3	+1.4	2.3×10^{-16}	+1.9	+0.8	2.1×10^{-17}	5000	2,1
BB	ε Aur	c F0	+3.4	+1.3	+2.1	6.0×10^{-16}	+1.2	+2.2	1.0×10^{-16}	7200	1,1

TABLE III
COMPARISON OF PERKINS AND MOUNT WILSON DATA

<u>Star</u>	<u>Perkins</u>		<u>Mount Wilson</u>		<u>Perkins</u>		<u>Mount Wilson</u>	
	<u>m_x</u>	<u>m_y</u>	<u>m_x</u>	<u>m_y</u>	<u>m_x</u>		<u>m_y</u>	
x9 α Cas	+0.1	-0.3	-0.4	+0.4	+0.5		+0.1	
14 β And	-2.0	-1.6	-1.8	-2.0	-0.2		+0.4	
20 γ And	-1.0	-0.4	-1.0	-0.9	0.0		+0.5	
21 α Ari		-0.3		-0.8			+0.5	
22 ο Cet	-3.0	-3.5	-3.0	-3.6	0.0		+0.1	
25 α Cet	-1.7	-1.4	-1.6	-1.8	-0.1		+0.4	
26 ρ Per	-1.9	-2.1	-1.9	-2.2	0.0		+0.1	
37 α Tau	-2.9	-2.9	-2.9	-3.0	0.0		+0.1	
41 ι Aur	-0.4		-0.8		+0.4			
136 α Boo	-2.2		-3.4		+1.2			
167 α Her	-3.5		-3.6		+0.1			
188 γ Aql	+0.1		-1.0		+1.1			
190 x Cyg	-2.3		-2.0		-0.3			
198 U Del	-0.9		-0.7		-0.2			
212 μ Cep	-2.1		-1.8		-0.3			
231 71 Peg	-0.4		-0.1		-0.3			
235 R Cas	-1.8		-1.3		-0.5			

catalogue number (Appendix IV) and the common designation of the star; the apparent magnitudes tabulated under the date upon which the individual measure was made; and finally the computed apparent magnitude of the star based upon the assumption that the stars radiate as blackbodies. Table I is presented in two parts, A and B, for the X-magnitudes and the Y-magnitudes, respectively.

In Table I are used several notations to indicate something of the quality of the observation or of the manner in which the magnitude determination was made. A single colon (:) following the tabulated magnitude indicates that the deflection used for the determination of that magnitude was not considered to be sufficiently steady or free from transparency or sensitivity changes to yield a reliable magnitude. A double colon (::) following a magnitude indicates that the observation was taken outside the time interval covered by blackbody reference signals which were used to monitor the sensitivity of the detector. As any reliance on these quantities would depend upon a rather drastic extrapolation of the sensitivity data, it was decided that these values would not be used in the determination of the mean values of the magnitudes entered in the summary of the Mount Wilson observations given in Table II. A magnitude enclosed in parenthesis () indicates that star used on that night as a standard star and the value is that obtained on another night by a direct intercomparison with the primary standard Vega (α Lyrae). A further discussion of the system of standards is given in Appendix II.

Table II consists of the mean values of the apparent magnitudes obtained on the nights listed in Table I. For many of the stars this value is the result of a single observation and there is no attempt to weigh these results in comparison to those stars for which there are four or more determinations of magnitude. An analysis of the mean deviations of the different observations of a given star indicates for the X-magnitudes an average deviation of ± 0.1 magnitude; for the Y-magnitude it is about ± 0.2 magnitude.

Of the eight long period variable stars observed, only four have reliably determined visual magnitudes for the nights upon which they were observed. These magnitudes are included in Table II under the column headed m_v and are enclosed in parentheses. The remaining long period variables have tabulated for their visual magnitude the maximum value listed for them in the Radial Velocity Catalogue (Reference 7).

The observed X- and Y-color indices are given in Table II as is the temperature for each star observed, based upon the temperature calibration given by Morgan and Keenan (Reference 5). This temperature is used to plot the observed colors against the theoretically calculated values, based upon the assumption that the stars radiate as blackbodies. Included are approximate values of stellar irradiances H_x and H_y . The final column of Table II gives, respectively, the number of observations used to determine the X- and the Y-magnitudes.

Figure 11, a plot of the X-index as a function of temperature, indicates a marked tendency for the points to lie above the theoretical curve for the coolest stars observed. Several of the points most removed from the theoretical curve are the variable stars observed far from the maximum light. These large indices are the result of the fact that the visual magnitude varies over a range corresponding to a light variation of two or more orders of magnitude while the temperature and presumably the infrared irradiance remains nearly constant. It is also significant that the non-variable stars at these temperatures also show a tendency to lie above the curve, which indicates that there may be some source of continuous opacity in the atmospheres of these stars which limits the amounts of visible radiation which can escape from the stars. Suggestions have been made that the formation of clouds of condensed molecular material may account for the wide variations in the visual brightness of the long period variable stars. It may be that a similar mechanism serves to decrease the visual irradiance of the non-variable stars in this temperature region although to a somewhat smaller extent.

Below a temperature of about 3000°K , the observed points seem to cluster about the computed curve. The only group of stars which seem in any way to show a consistent trend are the supergiant stars (represented by a (+) on the graph) which occur only above the curve at all temperatures.

The plots of observed minus computed values of X-color index for the supergiants and nonvariable giants are in Figures 13 and 14.

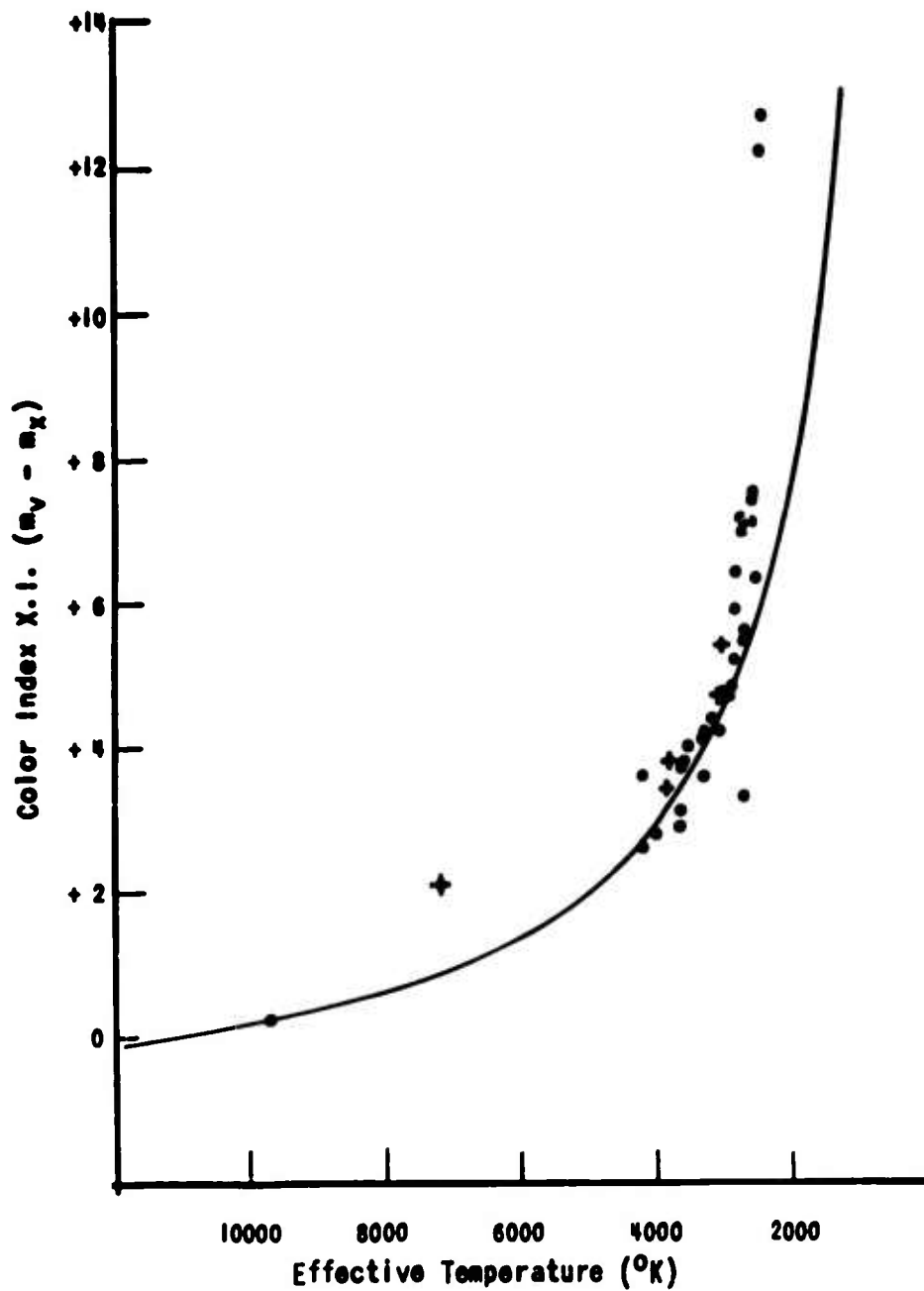


Figure 11. THE X-COLOR INDEX AS A FUNCTION OF TEMPERATURE

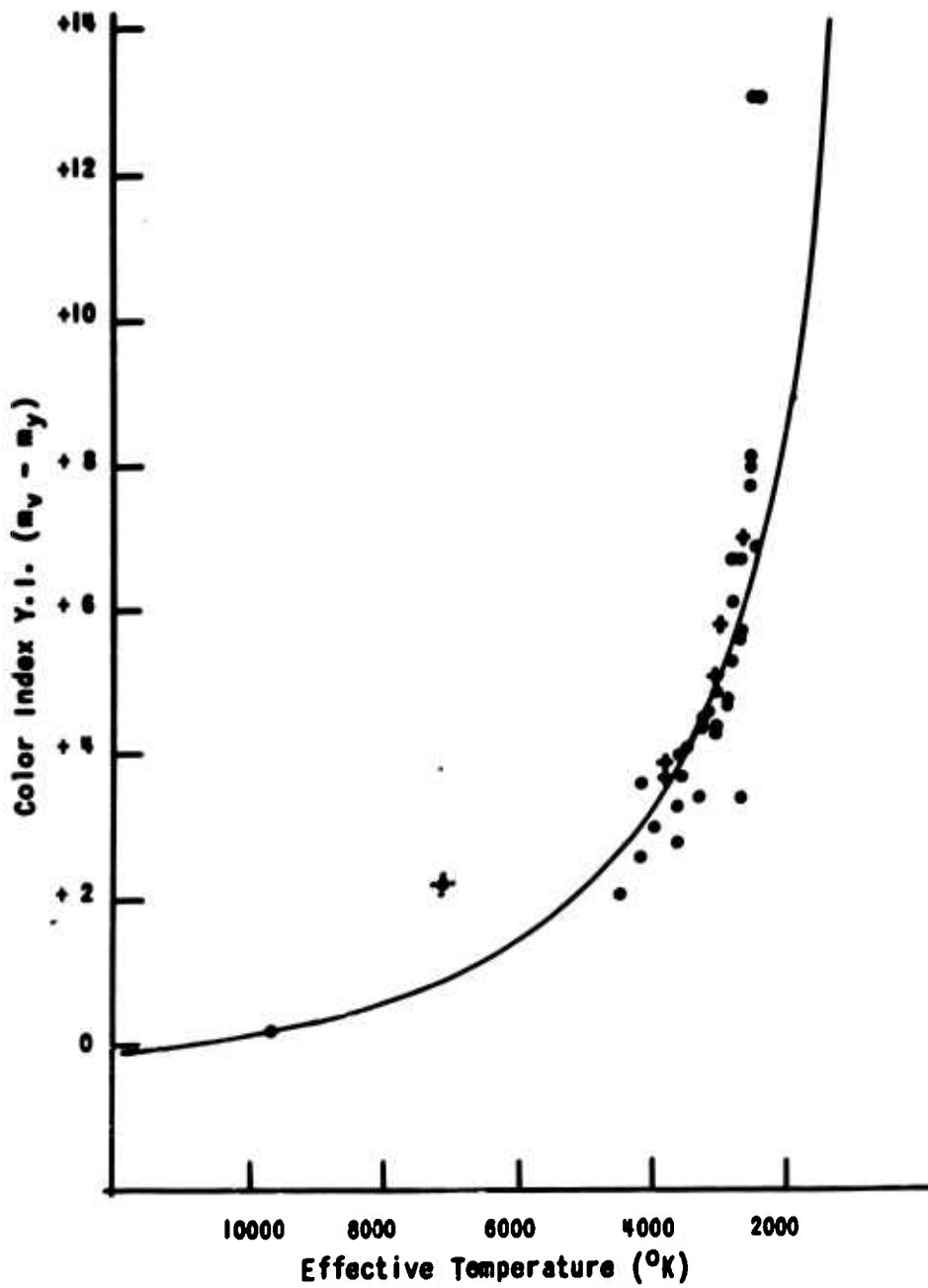


Figure 12. THE Y-COLOR INDEX AS A FUNCTION OF TEMPERATURE

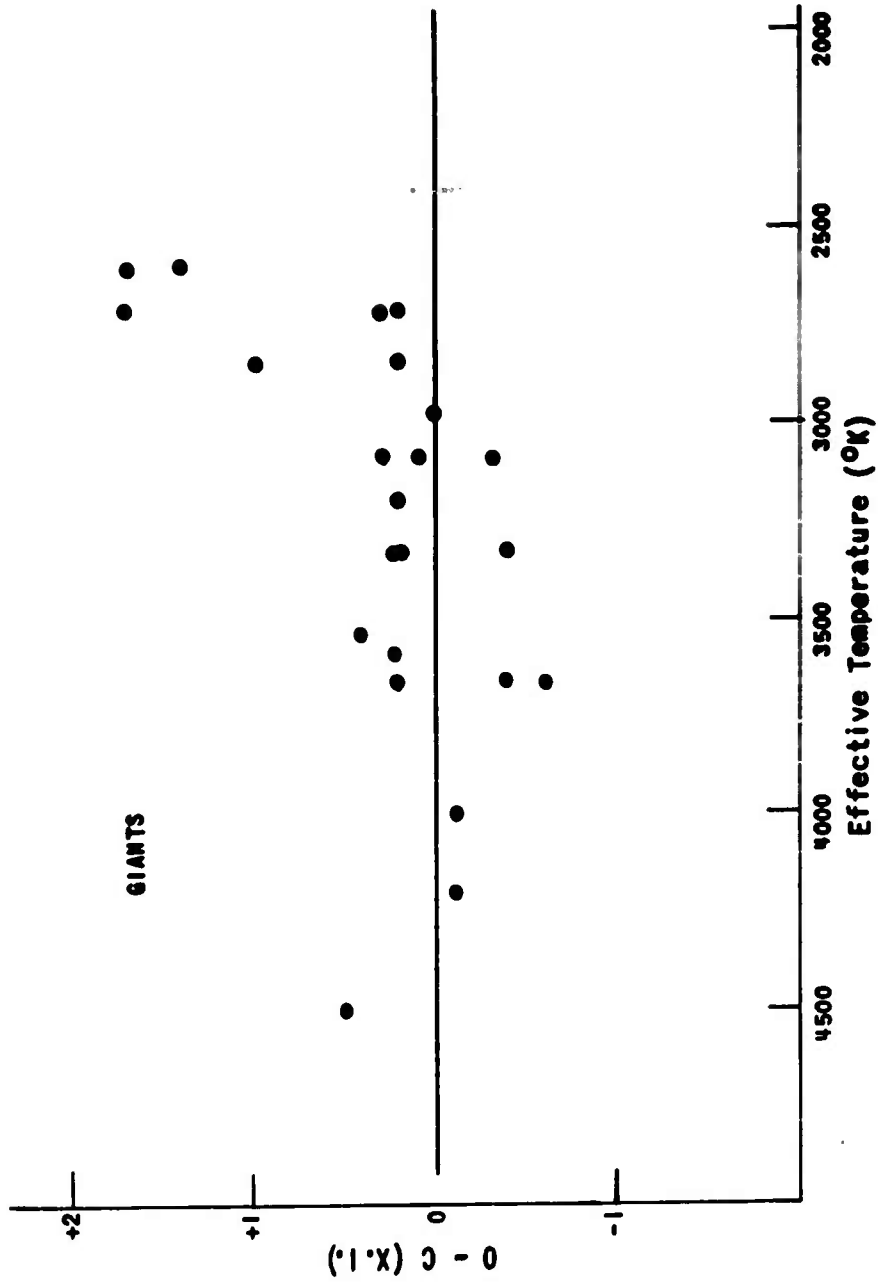


Figure 13. THE OBSERVED X- INDEX MINUS THE BLACKBODY CALCULATED X- INDEX AS A FUNCTION OF TEMPERATURE FOR NORMAL GIANTS

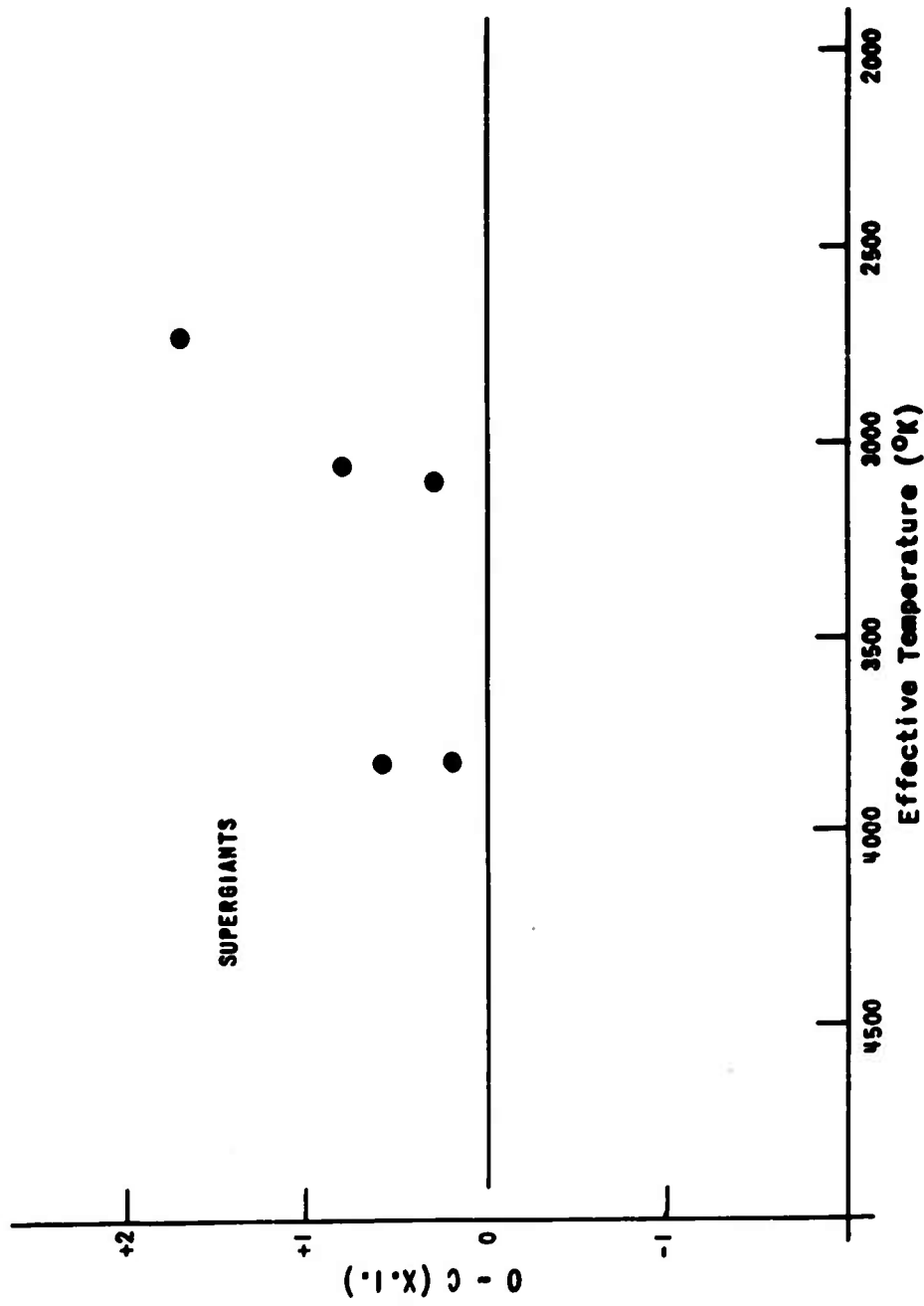


Figure 14. THE OBSERVED X- INDEX MINUS THE BLACKBODY CALCULATED X- INDEX AS A FUNCTION OF TEMPERATURE FOR SUPERGIANTS

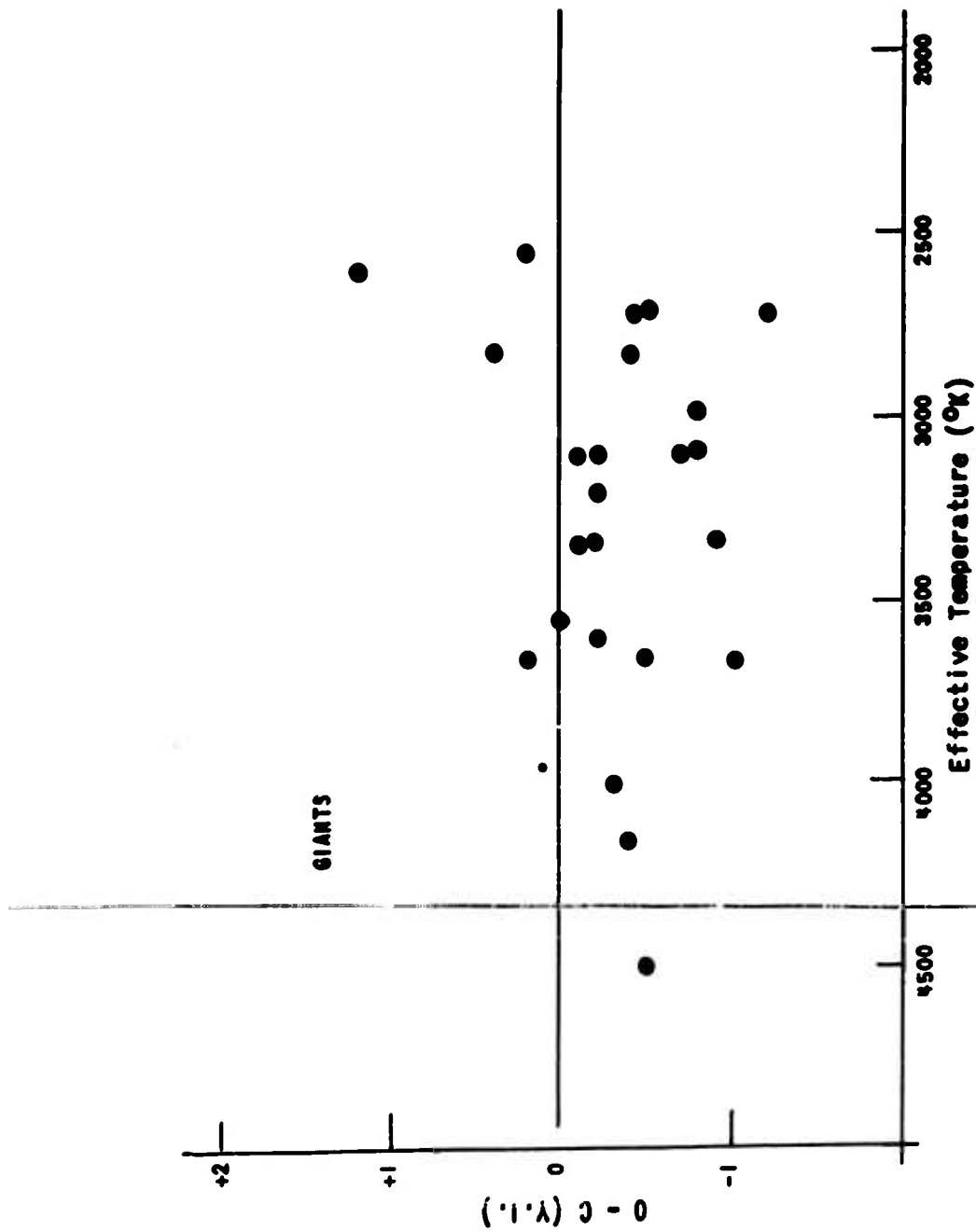


Figure 15. THE OBSERVED Y-INDEX MINUS THE BLACKBODY CALCULATED Y-INDEX AS A FUNCTION OF TEMPERATURE FOR NORMAL GIANTS

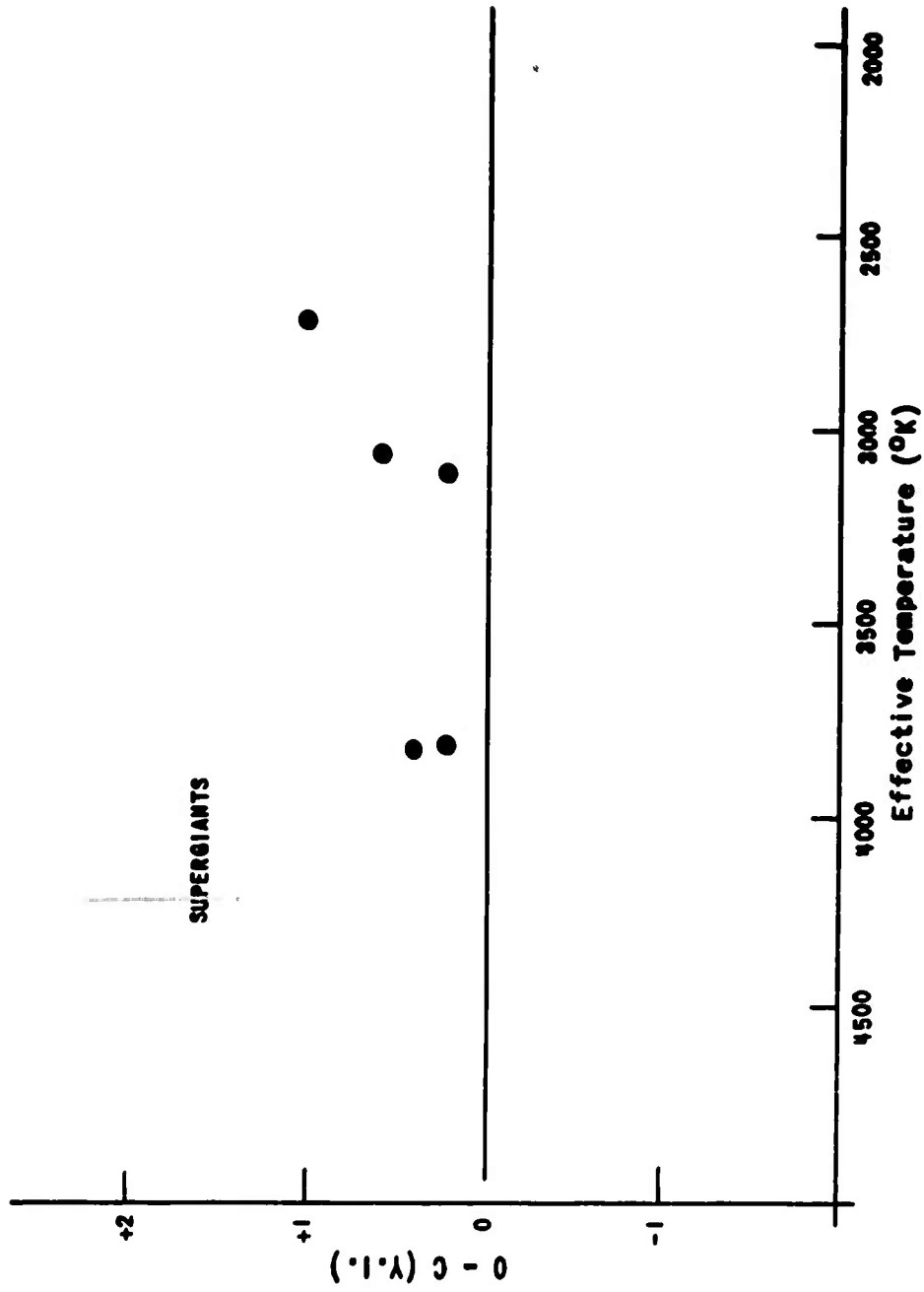


Figure 16. THE OBSERVED Y-INDEX MINUS THE BLACKBODY CALCULATED Y-INDEX AS A FUNCTION OF TEMPERATURE FOR SUPERGIANTS

The Y-indices plotted in Figure 12 show a similar trend to pass above the computed curve at temperatures below about 2500°K. It can be seen from the Y.I. curves, Figures 15 and 16, that the nonvariable stars cluster about a line about 0.5 magnitude below the predicted values. This is in essential agreement with some of the recent observations made by Freeman Hall (Reference 4).

The supergiants show a tendency in the Y-band to again lie systematically above the computed curve. It seems apparent that the supergiant stars possess an excess of infrared radiation emission in the wavelength bands which we have studied. The combination of the two results just mentioned; i.e., the excess infrared emission of both the supergiants and the very latest spectral type stars, would lead one to underestimate the severity of the background problem if the assumption of blackbody radiation is used. The amount of underestimation on the basis of the supergiants alone would represent a factor of about 5 in the numbers of such stars which would be detectable. As there are relatively few of these stars in a given volume of space this need not be considered a serious problem. There are however many more very cool giant stars which show an excess of the infrared radiation. It would seem that more study is indicated for these objects in terms of the nature of the excess and possible modification of the temperatures for these stars. It must be pointed out here that many of the very coolest stars on this program are plotted for temperatures which were of necessity extrapolated from the

temperature data of Morgan and Keenan. There is reason, therefore, to suppose that corrections to the assumed temperature scale for these cool stars may be justified.

The temptation to modify the temperature scale for any of these late type stars should be suppressed until the degree of blanketing in the visual region is more fully investigated. There is also need for a more detailed study of molecular absorption in the infrared which may have a direct bearing upon the determination of strictly IR color indices, e.g., $(m_x - m_y)$. Such indices obtained with very accurate X- and Y-magnitudes could be used to provide accurate color temperatures for the late type stars.

F. CONSIDERATION OF THE ABNORMAL OBJECTS

So far we have described only the normal stars in which were included the long period variable stars whose behavior is not particularly stable but at least predictable. There were in addition to these stars three others observed which deserve some additional and special comment. These stars are; T Corona Borealis, X Aquarii, and ϵ Aurigae.

T Corona Borealis (T CrB) was included on the list of bright objects which should be easily observable with the infrared photometer. With a computed magnitude of about -3.0 for each wavelength band it lies about 6 magnitudes above the limit of the photometer. Attempts were made on two nights to obtain infrared deflections for this star in both the X- and Y-bands without success. A look into the nature of this object indicates that it is

not of the typical long period variable type and indeed seems to possess some features that are entirely at variance with those of the long period variables. The nature of the variation of T CrB is such that the star in its "normal" state is at about 9th or 10th visual magnitude. Occasionally the star flares up to nearly 2nd magnitude, such occurrences giving to the star its popular name "the Blaze Star".

The calculation of the infrared magnitudes were made on the basis of the maximum magnitude. The result of this arbitrary treatment of the variable stars produced an infrared magnitude about 7 or 8 magnitudes brighter than the star actually possesses. Other stars of this type, when they are encountered, should be treated as if their normal state is that of minimum visual magnitude.

X Aquarii (X Aqr) is another variable star which revealed an unexpected result. At a temperature of about 2700° , the calculated X-magnitude is -0.2 and the Y-magnitude is -0.7. The observed X- and Y-magnitudes respectively are +1.8 and +1.7. This represents a deficiency of 2.0 and 2.4 magnitudes in the X- and Y-bands. The observed values are obtained from observations made on two nights and, though they were taken at fairly large zenith distances, such deviations from the computed values have not been observed for any other star. The reason for this abnormally low irradiance is not apparent.

During the course of the program of photometry of the late type stars observations were made of the eclipsing binary ϵ Aurigae (ϵ Aur) in both the X- and Y-wavelength regions. These data are given below with calculated colors and magnitudes based upon the assumption of blackbody emission of a single star of the spectral type of the primary component of ϵ Aurigae:

<u>Spectral Type</u>	<u>F0 V (plus a nonvisible companion)*</u>	<u>Remarks</u>
m_v	+3.4	Wilson (Reference 7)
m_x	+1.3	EK/OSU Infrared Stellar Photometer, Mount Wilson Observatory, August, 1961
m_y	+1.2	
X. I. ($m_v - m_x$)	+2.1	
Y. I. ($m_v - m_y$)	+2.2	
m_x (calculated)	+2.6	Blackbody assumption for F0 I star alone T = 7200°K
m_y (calculated)	+2.6	
T (IR)	1350°K	Kuiper, et al, Reference 6
log R (IR)	+3.43	
log Mass (IR)	+1.39	

* Kuiper, et al (Ref. 6)

In their description of the binary system ϵ Aurigae, Kuiper, Struve, and Stromgren (Reference 6) depicted a normal F type supergiant accompanied by a large cool star which eclipses the F star every 27 years. The cool component with a derived temperature of 1350° does not emit enough visible radiation to be noticed even during the primary eclipse. As the primary eclipse is evidently only an atmospheric eclipse there seems to be no possibility that a secondary minimum can be detected in the visible region.

If the companion of the F supergiant is indeed a star of such low temperature, most of its energy will appear in the infrared and it thus becomes an object of interest in any program of infrared stellar photometry. When it was noted that the measured infrared magnitudes of ϵ Aurigae were more than one magnitude brighter than predicted on the basis of the F-component alone, efforts were made to determine if the excess infrared radiation could be reconciled with an object of the type described by Kuiper, Struve and Stromgren.

Taking the observed apparent Y-magnitude to be the combined magnitude of the system, and the calculated apparent magnitude for the F0 I star to be +2.6, ($m_v - YI_{\text{calc}}$), it is found that the apparent Y-magnitude of the infrared component alone is +1.6.

The distance of ϵ Aurigae is given by Kuiper et al (1937) as 1000 parsecs. This provides an absolute Y-magnitude of -8.4. From Appendix III the Y-luminosity of a star with $M_y = -8.4$ is 8.4×10^{27} watts.

The radius of a blackbody emitter required to produce the observed Y-luminosity as a function of temperature has been computed as follows:

Temperature (°K)	Radiant Energy of Blackbody (3.2 to 4.2 microns) (watts/cm ²)	Surface Area (To produce M _y = 8.4) (cm ²)	Radius (cm)
820	0.47	1.8 x 10 ²⁸	3.8 x 10 ¹³
1000	1.1	7.6 x 10 ²⁷	2.5 x 10 ¹³
1350	3.6	2.3 x 10 ²⁷	1.4 x 10 ¹³
3100	26.	3.2 x 10 ²⁶	5.2 x 10 ¹²

The published radius of the infrared component of ϵ Aurigae is 1.9×10^{14} cm, about one order of magnitude greater than the calculated size of a 1350° blackbody as shown above. However, from the photometric observations in the visible region of the spectrum it would seem the outer layers of the star are fairly transparent, producing a primary minimum of only 0.3 magnitude. We might thus picture a star with an infrared photosphere at the effective temperature of 1350° and having about 1/10 the radius of the atmosphere. If the atmosphere of the infrared component proves to be quite opaque to the infrared radiation of the FO component, thereby showing its nearly blackbody character, then we would be led on the basis of the size determination of the star to conclude a much lower temperature than 1350°.

It becomes of great interest then to measure the variation of the infrared irradiance during the next eclipse of the system to see just how opaque the atmosphere is to the infrared radiation of the FO star. Since the apparent Y-magnitude of the IR component alone is +1.6 and the Y-magnitude of the system is +1.2 we would expect on the basis of a totally opaque atmosphere a decrease of the Y-magnitude of 0.4 as the FO star passes behind the atmosphere of the infrared component. If the decrease in infrared brightness is any less than this or if the FO component passes behind the atmosphere of the infrared star without a decrease in the Y-irradiance, we would then be certain that the outer layers of the star do not behave in the manner of a blackbody in the infrared and that the majority of the infrared radiation probably comes from a somewhat smaller photosphere which does not participate in the eclipse.

If we assume a star of absolute Y-magnitude of -8.4 at a distance of 1000 parsecs it is possible to calculate the visual irradiance of the same star if it radiates as a blackbody. For a 1350° blackbody, the Y-irradiance is about 700 times the visual irradiance. Thus a star having $m_y = +1.6$ and an irradiance at the earth of 7×10^{-17} watts/cm² in the Y-band (Reference 2) will have a V-irradiance* of $(1.1 \times 10^{-4})I_y$ or 7.7×10^{-21} watts/cm². This corresponds to a visual magnitude of $m_v = +19.2$. In combination with the FO component the infrared star contributes essentially nothing to the visual magnitude of the system.

* Visual irradiance

The observation of a "truly infrared" star in the system of ϵ Aurigae makes it all the more important to try to identify such objects in the vicinity of the sun. Consider an infrared star of this type in the vicinity of the sun, for instance, at 20 parsecs (instead of 1000 parsecs). It would have a visual magnitude of +10.7 but a Y-magnitude of -6.9. Such a star, though visually 100 times fainter than the faintest naked-eye star, would have an infrared brightness seven times that of Betelgeuse, which is itself the eighth brightest naked-eye star. Even at this close range the linear extent of the star's enormous disk would be well beyond the resolving power of the largest telescope.

Two methods suggest themselves for the detection of such objects: (1) photographic, at wavelengths 0.4-0.9 microns, wherein they would exhibit large color indices, and (2) infrared scanning with a wide-field instrument of moderate to high sensitivity.

APPENDIX I

NOTES ON MOUNT WILSON DATA REDUCTION

1. Raw data was taken from the tapes in the form of net deflection, (star deflection minus sky deflection) as follows:

Time of observation
Star identification
Filter used
Net deflection
Gain setting
Hour angle (if recorded)
Temperature when recorded
Blackbody Deflections

2. The blackbody deflections and star deflections were then normalized to gain 19, the highest gain setting available. This was accomplished by using the input attenuator calibration labelled "Normalized Factor". This served to place the observations on a common basis for determining relative intensities.

3. It was noted that the blackbody deflections, presumed to have been taken from a constant temperature source, varied in some cases by factors of 3 or 4, over the period of time covered by the observation.

This has been interpreted as a variation in detector sensitivity; although the exact cause is unknown, it has been treated as if there has been introduced at each point during the night an arbitrary gain or attenuation factor.

The determination of this factor would have been very straightforward had the blackbody comparisons been made at the time of each star observation. Unfortunately the variation in blackbody deflection was not recognized at the time of observation and it was not considered necessary to take blackbody comparisons more than about once an hour.

As a result it has become necessary to make certain assumptions concerning the variation of system sensitivity between the measured blackbody points as well as some of the regions outside the measured points.

The normalized blackbody deflections are plotted as a function of time.

- a. The variation of sensitivity between points on the graphs is assumed to be continuous and smooth.
 - b. No attempt has been made to infer peaks or dips between points although there may be evidence of such in the reduced data.
 - c. Extrapolation has not been carried out more than a small fraction of an hour beyond end points. Objects having magnitudes determined from extrapolated sensitivity data have such magnitudes marked with a double colon (::) on the summary sheets. Correction factors, termed "sensitivity factors," were obtained from the smooth blackbody deflection versus time curves which were then used to convert the star deflections to sensitivity comparable to that of the system at the time the standard star was measured. This technique in essence smoothed the assumed blackbody curve to a flat curve through the point corresponding to the sensitivity at the time of the observation of the standard stars.
4. Application of the sensitivity factor to the normalized deflections yields the value L^* , taken to be proportional to the intensity of the radiation in the appropriate wavelength band.
5. Ratios are taken between the L^* for the stars and the standard star chosen for the appropriate time interval. These ratios (L^*/L_0) are then converted to differences in stellar magnitude between the stars and the chosen standard.
6. By application of the standard star magnitude it is then possible to arrive at the X- and Y-magnitude of each star.
7. These magnitudes are tabulated on the summary sheets in Appendix V.

APPENDIX II
COMMENTS ON STANDARD STARS

In view of the uncertain nature of all the stars on the program it was decided to use as few standard stars as possible; that is, to observe the magnitude difference of the program stars with respect to the same star as often as possible. The following considerations were deemed important in establishing the magnitude system.

1. The zero point of the m_y and m_x magnitude scales should be set by observations on a star as near in spectral type as possible for the spectral type used to set the zero point in the theoretical calculations of the infrared color systems. This type is A0 V and the only star observed this summer near this spectral type is Lyrae at A2 V.
2. Since α Lyrae could not be observed on every night, due for instance to clouds in the early part of the evening, a secondary standard (or standards) should be set up to fulfill as many of the following requirements as possible.
 - a. It should be a well observed star; i.e., a star which has a magnitude determined on several nights.
 - b. It should lie somewhere in the middle of the region of the sky being observed so that a minimum of time difference occurs between the observation of the standard and the star being measured.
 - c. It should be relatively bright.
 - d. It should have a magnitude well determined with respect to α Lyrae, the primary standard.

One star which was observed on most nights was β Pegasi. Besides being a star well observed during the previous fall and winter, it is a bright star producing large reliable deflections.

There are however several drawbacks to the choice of β Peg. Though it was observed on four nights with α Lyrae, only two can be used for direct comparison.

<u>Date (1961)</u>	<u>Remarks</u>						
Aug 15-16	Detector change occurred between observation of α Lyr and β Peg.						
Aug 16-17	Whole night referred to α Lyr. There is some question as to the sensitivity correction for the time α Lyr was observed. This night might better have been referred to β Peg alone.						
Aug 17-18	Direct comparison: β Peg/ α Lyr <table style="margin-left: 200px;"> <tr> <td>m_x</td> <td>=</td> <td>-2.2</td> </tr> <tr> <td>m_y</td> <td>=</td> <td>-2.3</td> </tr> </table>	m_x	=	-2.2	m_y	=	-2.3
m_x	=	-2.2					
m_y	=	-2.3					
Aug 19-20	α Lyr was 4 1/2 hours west when observed and atmospheric effects were uncertain. Only R Lyrae measured at same time, was referred to α Lyr.						

On the basis of the one reliable intercomparison of α Lyrae and β Peg, it was decided to consider the values of the magnitudes for β Peg as:

$$m_x = -2.2$$

$$m_y = -2.3$$

These values were both measured for the two stars on August 17-18, 1961. The value for m_x is about 0.4 magnitudes brighter than the calculated value from the theory, but the value for m_y is the same as the theoretical determination.

As there is no way to determine the relative brightness of the star from one night to the next, independent of the sensitivity corrections, there is no way of telling how reliably the observations of β Peg can be reproduced.

In spite of the inherent danger of using β Peg for a standard, it is to be noted that there is no other star which fits the requirements set down above any better than does β Peg. Therefore, with one exception, this star was used as a secondary standard at all times when α Lyr was not available. The one exception was the use of α Ceti on August 20-21, 1961 for the stars observed with detector D-5 for which there were no deflections of β Peg made. This star was chosen at the time because it was thought to be the best observed of those under consideration. α Ceti might have been as good a choice but, due to the fact that it is known to be a long period variable star, it was decided that it would be best not to rely upon it for standardization.

APPENDIX III

THE INFRARED CHARACTERISTICS OF PROTOSTARS AND DARK GLOBULES

by
Philip E. Barnhart
Perkins Observatory, Delaware, Ohio

INTRODUCTION

Since the application of high-sensitivity IR detectors to the field of stellar photometry, much interest has arisen in the possibility of measuring irradiances of various objects in space which do not emit visible radiation (0.4 to 0.7 micron) but which, due to their temperature or size, may emit considerable amounts of radiation in the longer wavelengths. Pressure is being applied by theoretical astrophysicists to attempt the detection of contracting protostars, the existence of which is strongly supported by theoretical considerations of the requirements of star formation and the observational evidence of the presence of such objects in very young galactic clusters. Interest is also being shown in the fairly numerous, dense, dark globules of interstellar material which appear silhouetted against luminous nebulae or star clouds as possible breeding grounds for these protostars.

The present calculations are concerned with the infrared characteristics of certain assumed types of protostars and the potential IR results based upon observed characteristics of dark globules. These calculations are based upon the experimental results on normal stars in the plumbide region (3 to 4 microns) for two reasons.

1. Astronomical performance characteristics of the plumbide cell are well known so we can work from a well established limiting detectability.

2. For the intermediate temperatures encountered in pre-main sequence contraction (800° to 2000°), the plumbide sensitivity is centered nearer the energy peak than that of the copper-doped germanium detector.

OBSERVATION OF PROTOSTARS

Observations of galactic clusters in recent years have demonstrated the fact that cluster ages may be determined with fair accuracy by observing the brightest cluster members still existing on the main sequence. The luminosity thus obtained, coupled with the rate of mass to energy conversion for a "zero-age" star at that position on the main sequence, yields an age of the cluster, assuming all stars in the cluster "formed" at the same time.

Certain clusters showing memberships consisting in part of very luminous O and B stars whose ages, because of their very high luminosities, must be very young (less than 500,000 years in some instances) led M. F. Walker (Ref. 1-4) to make photometric studies of the fainter stars in these clusters in hopes of detecting stars still in their pre-main sequence contractions. These stars will not be emitting energy generated by thermonuclear reactions in the core, but will be radiating mostly energy generated by the process of gravitational contraction first described by Helmholtz in 1854. Walker has indeed detected such protostars in 4 young clusters.

If the energy radiated as well as the temperatures possessed by such stars comes about as the result of the physical contraction of the body, the supposition would be that the cooler body would, in general, be larger in size than the body arriving at the main sequence, where the star's central temperature is just high enough to maintain the thermonuclear reactions necessary to establish the given mass as a stable star. This state is one in which the gravitational attraction inward is just balanced by the

gas and radiation pressure outward resulting from the internal energy generation, and the main sequence represents the locus of points in the H-R diagram corresponding to such stable stars of different initial mass.

Studies of Helmholtz contraction indicate that the temperature of a contracting mass, assuming homologous contraction, will vary inversely as the radius of the object (Ref. 5).

Calculations of late phases of gravitational contraction based upon the Helmholtz temperature increase have been carried out by Schwarzschild and others for objects of various masses. These calculations extend backward from the zero-age main sequence to points where the temperature just places the star at the cool end of the H-R diagram, which means a temperature within a factor of 2 or 3 for the sun or a factor of about 8 for a star of 10 solar masses. Attempts to extrapolate much further on the contraction hypothesis may possibly lead to serious errors due to a decrease in the opacity of the contracting cloud at such low densities. Extrapolations of temperatures by factors of 100 and 1000 are considered, however, in the present calculations to obtain order-of-magnitude values for small contracting clouds of the order of a few solar masses. Table A indicates the surface areas and temperatures of 3 "protostars" with masses of 1, 5, and 10 times the mass of the sun. On the basis of an inverse dependence of temperature on the radius an increase of a factor 10 in temperatures will be produced by a decrease in the radius by the same factor.

TABLE A

<u>Mass</u> <u>Solar Masses</u>	<u>Main Sequence</u> <u>Sp. T.</u>	<u>Temp.</u> <u>°K</u>	<u>Helmholtz</u> <u>Temp.</u> <u>°K</u>	<u>Surface</u> <u>Area</u> <u>cm²</u>	<u>Radius</u> <u>cm</u>
1	G2	6000	6000	8.8×10^{21}	7×10^{10}
			600	8.8×10^{23}	7×10^{11}
			60:	8.8×10^{25}	7×10^{12}
			6:	8.8×10^{27}	7×10^{13}
5	B8	15400	15400	3.3×10^{23}	2.4×10^{11}
			1540	3.3×10^{25}	2.4×10^{12}
			154:	3.3×10^{27}	2.4×10^{13}
			15.4:	3.3×10^{29}	2.4×10^{14}
10	B0	22400	22400	4.4×10^{23}	3.5×10^{11}
			2240	4.4×10^{25}	3.5×10^{12}
			224:	4.4×10^{27}	3.5×10^{13}
			22.4:	4.4×10^{29}	3.5×10^{14}

If we know the surface area and temperature of a body, it is then possible to determine the luminosity, either total or in a particular wavelength region if we assume the object radiates as a blackbody. In order to do this for the 3-4 micron region, a group of significant temperatures was selected to provide an indication in what direction the observations might tend.

1. 820°K - The temperature at which the blackbody curve peaks at 3.5 microns, the center of the 3-4 micron band.

2. 1300°K - The temperature at which the blackbody curve peaks at 2.25 microns (center of the lead sulfide region, 2.0-2.5 microns), and also near the temperature at which a maximum percentage of the total radiation falls within the 3 to 4 micron band.
3. 3100°K - The temperature of Betelgeuse, used to directly compare the detectivity in terms of an object of known luminosity.

The spectral characteristics of the three temperatures are summarized in Table B.

TABLE B

<u>T</u> <u>(°K)</u>	<u>λ max.</u> <u>(micron)</u>	<u>Total Radiant</u> <u>Energy</u> <u>(watts/cm²)</u>	<u>Fraction in</u> <u>3-4 microns</u>	<u>Radiant Energy</u> <u>3-4 microns</u>
820	3.5	2.6	0.18	0.47
1300	2.25	16.0	0.20	3.2
3100	0.93	520	0.05	26.0

With the data of Tables A and B it is now possible to compute the Y-luminosities of the selected protostars at the chosen temperatures. Before doing this, it may be well to establish the limiting Y-irradiance detectable with the nitrogen cooled plumbide detector.

LIMIT OF DETECTABILITY

During the observing program carried out with the photometer on the 100-inch telescope, the faintest signal measured was due to ϵ Cephei at an apparent magnitude, $m_y = +2.9$. This corresponded to an apparent irradiance, $h_y = 2 \times 10^{-17}$ watts/cm². On this basis we can tabulate the absolute Y-magnitude M_y , which will produce the apparent irradiance (10^{-17} watts/cm²) at the earth from a given distance. This is obtained from the relation:

$$M_y = m_y + 5 - 5 \log r$$

where $m_y = +3.5$

TABLE C

<u>r</u> (parsecs)	<u>log r</u>	<u>M_y</u>
1	0	+ 8.5
10	1	+ 3.5
100	2	- 1.5
1000	3	- 6.5
10000	4	-11.5

M_y - absolute Y-magnitude of a star which is just detectable from a distance, r.

To calibrate our magnitude scale in terms of apparent irradiance, we need but one object of known apparent magnitude and distance. The most reliably determined apparent magnitude in the Y-region is α Orionis, the brightest star observed with the experimental photometer.

The pertinent data for α Ori is as follows:

Distance (Ref. 6)	$r = 200$ parsecs
Apparent Y-Magnitude	$m_y = -5.0$
Apparent Y-Irradiance	$h_y = 3 \times 10^{-14}$ watts/cm ²

The absolute magnitude is then:

$$\begin{aligned}M_y &= -5.0 + 5.0 - 5 \log 200 \\ &= -5(2.3) \\ &= -11.5\end{aligned}$$

This gives the distance modulus:

$$(m_y - M_y) = +6.5$$

To determine the "Absolute" irradiance, H_y (= the irradiance at the earth if α Orionis were at a distance of 10 parsecs) we need the relation:

$$\begin{aligned}\log \frac{H_y}{h_y} &= 0.4 (m_y - M_y) \\ &= 0.4 (6.5) \\ &= 2.60\end{aligned}$$

thus:

$$\begin{aligned}H_y &= 400 h_y \\ &= 1.2 \times 10^{-11} \text{ watts/cm}^2\end{aligned}$$

A plot of apparent irradiance, (h_y), or apparent magnitude m_y , as a function of distance, r (in parsecs), for objects with various absolute magnitudes, M_y , is shown in Figure III 1.

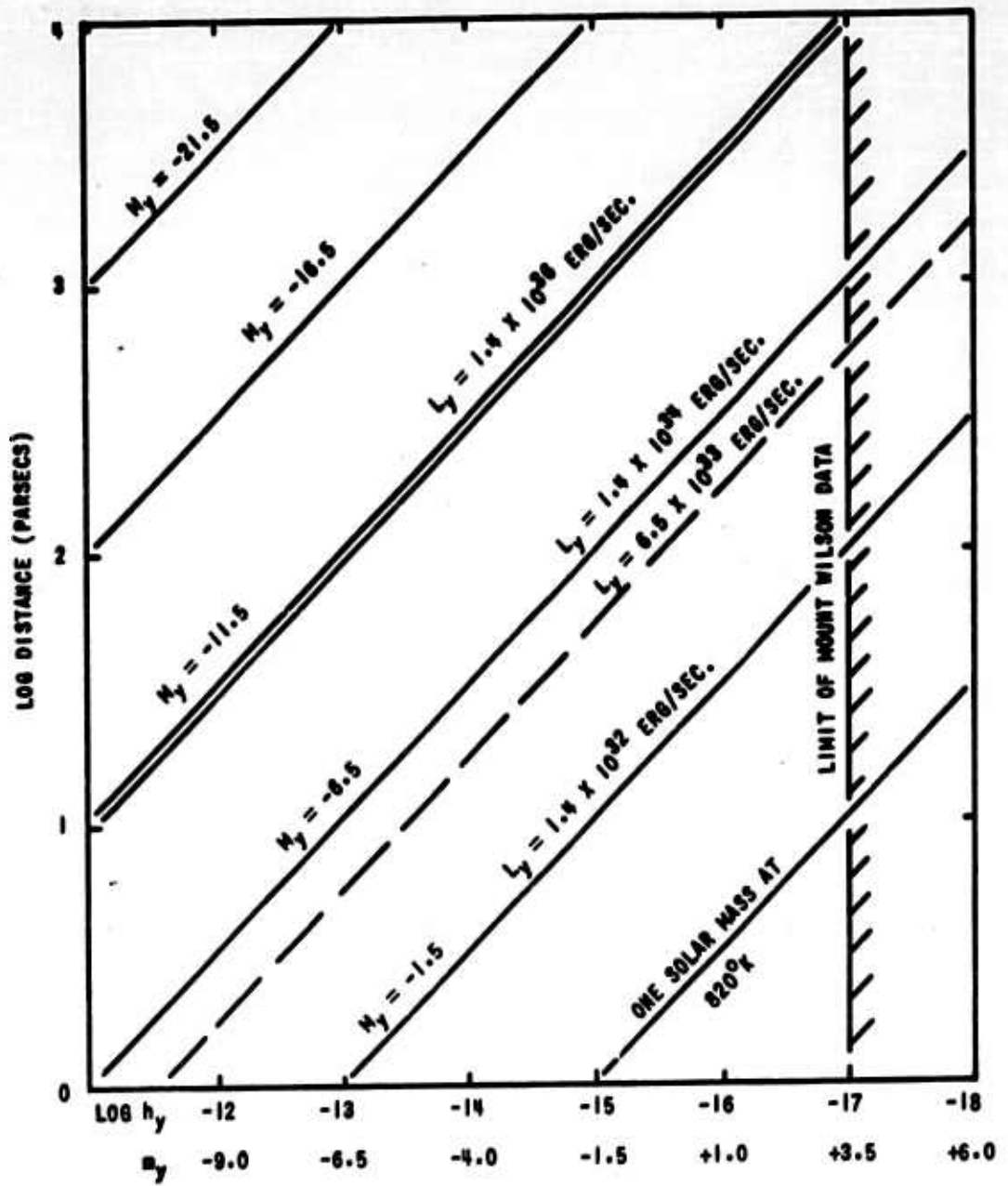


Figure III-1. APPARENT IRRADIANCE OF OBJECTS HAVING VARIOUS MAGNITUDES AND DISTANCES

If we compute the Y-luminosity of α Orionis, then we will be able to determine the absolute irradiance for any object whose luminosity and distance is known.

The temperature of α Ori is 3100° so the total power radiated per square centimeter of surface, assuming emissivity = 1.0, is given by the Stefan-Boltzmann law:

$$\begin{aligned} E &= \sigma T^4 \\ &= 5.2 \times 10^2 \text{ watts/cm}^2 \end{aligned}$$

of which 5% falls in the 3 to 4 micron band. Therefore

$$E_y = 26 \text{ watts/cm}^2$$

The radius of α Ori is 295 times the radius of the sun, (Ref. 8), or:

$$\begin{aligned} R_B &= 295 (7 \times 10^{10} \text{ cm}) \\ &= 2.06 \times 10^{13} \text{ cm,} \end{aligned}$$

for which the surface area is:

$$\begin{aligned} A &= 4\pi r^2 \\ &= 5.35 \times 10^{27} \text{ cm}^2 \end{aligned}$$

and at 26 watts/cm² this gives a luminosity of:

$$\begin{aligned} L_y &= 1.39 \times 10^{29} \text{ watts} \\ &= 1.4 \times 10^{36} \text{ ergs/sec} \end{aligned}$$

This value of the Y-luminosity agrees with the value obtained from the ratio of the blackbody energies in the visual and Y regions of the spectrum and the visual luminosity of the star.

Thus an object with an IR luminosity of 1.4×10^{36} ergs/sec will have an absolute Y-magnitude of $M_y = -11.5$ and will just be detectable from a distance:

$$\begin{aligned}
\log r &= 1 + \frac{(m_y - M_y)}{5} \\
&= 1 + \frac{(3.5 + 11.5)}{5} \\
&= 1 + 3.0 \\
r &= 10000 \text{ psc}
\end{aligned}$$

With this information the maximum distance at which any object whose luminosity can be computed can be determined. The luminosity calibration has been included on the plot of Figure III-1 and labelled, L_y .

LUMINOSITY OF PROTOSTARS

If we now compute the luminosity of the various individual protostars described above, we can get an idea of the maximum distance at which this particular type of object can be observed.

From the temperature-radius data of Table A, it is possible to determine the surface area of each model protostar at the temperatures of interest. This, combined with the data of Table B, will provide the luminosity of each contracting body at each significant temperature. This is tabulated in Table D.

TABLE D

Temp. (°K)	<u>1 Solar Mass</u>		<u>5 Solar Masses</u>		<u>10 Solar Masses</u>	
	Area (cm ²)	L_y (watts)	Area (cm ²)	L_y (watts)	Area (cm ²)	L_y (watts)
820	4.8×10^{23}	2.2×10^{23}	1×10^{26}	4.7×10^{25}	3.5×10^{26}	1.6×10^{26}
1300	1.8×10^{23}	5.8×10^{23}	4×10^{25}	1.3×10^{26}	1.5×10^{26}	4.8×10^{26}
3100	3.5×10^{22}	9.1×10^{23}	8×10^{24}	2.1×10^{26}	2.5×10^{25}	6.5×10^{26}

As can be seen from Table D, the brightest possible case is the 10 solar mass protostar at a temperature of 3100°K. This object will then already be on the H-R diagram so cannot be considered an "unknown" object. However, if we plot such an object on Figure III-1, we will have an upper limit of the distance to which a small, discrete contracting protostar can be observed. The broken lines in Figure III-1 represent this upper limit to the detectivity of protostars. A look at Table D shows that, in general, the contracting mass has a much smaller radius at a temperature of 3100°, than a supergiant star like α Ori. Thus, we might expect individual protostars of less than 10 solar masses to be detected in the Y-region at distances up to 1000 parsecs. The nearest of Walker's young clusters (NGC 2264) is 800 parsecs from the sun.

The preceding calculation is based upon the assumption that stars form as individuals out of clouds having essentially the mass of the final product star on the main sequence. Such is most likely not the case. Where very young stars are found they are usually found in groups (open clusters, O associations, T associations) of apparent common origin and nearly common age. Thus, it would seem that the proper method of star formation might involve the condensation of a cloud of interstellar material of considerably greater mass than a single star and one which will fill a greater volume of space at a given temperature than one of smaller mass content, and thus have a much greater surface area from which to radiate at a given rate for a given temperature.

The question now becomes: what sort of object at the distance of the farthest young cluster studied by Walker (NGC 6611, $r = 3.3$ kiloparsecs) would be required to be observable at the earth ($h_y = 10^{-16}$ watts/cm²)? A glance at Figure III-1 reveals that at the limit of detectability at 3.3 kpc a luminosity equal to that of α Orionis is required; that is, $M_y = -11.5$. So any object to be observed at this distance must have a luminosity in the 3-4 micron region of

$$L_y > 1.4 \times 10^{36} \text{ erg/sec}$$

TABLE E

Temp. °K	Rad. Energy (3-4 mic) ergs/sec/cm ²	Area cm ²	Radius		
			cm	Sun = 1	A.U.
820	4.7×10^6	3×10^{29}	1.1×10^{15}	1.64×10^4	73
1300	3.2×10^7	4.4×10^{28}	1.4×10^{14}	2.4×10^3	9.5
3100	2.6×10^8	5.4×10^{27}	2.1×10^{13}	2.9×10^2	1.4

In terms of astronomical sizes, the values given in the last column of Table E are quite moderate. For the coolest object this is a radius about twice the radius of the solar system. For 1300° the radius is the same as the radius of the orbit of Saturn, while α Orionis has a radius just under the radius of the orbit of Mars.

On a published photograph of NGC 6611 (Ref. I) a nearly circular "dark globule" can be seen projected against the bright nebulosity associated with the cluster. According to the published plate scale, the globule has a diameter of 17.4 seconds of arc, which, at a distance of 3.3 kps, amounts to 5.8×10^4 astronomical units. This rather typical blob then has a total surface area of about 9.6×10^{36} cm². In order for this object to have a total luminosity of 1.4×10^{36} erg/sec, it must emit 0.146 ergs/sec/cm² ($= 1.46 \times 10^{-8}$ watt/cm²). This rate of emission will occur for a body of this size at about 150°K. It seems quite reasonable to suppose that if material has condensed to a state where it is optically thick, that perhaps it has utilized enough gravitational energy to raise its temperature a few hundred degrees above the temperature of interstellar space (3.5°K). Also, being in the vicinity of highly luminous O and B stars, the back side of the cloud may absorb a considerable quantity of ultraviolet radiation from these stars, raising the temperature above the mean temperature of interstellar space.

If the globules were to reach a temperature, by any means whatever, of 820°K, they would then have a total luminosity of 2×10^{44} ergs/sec. This would produce a y-luminosity of 4.5×10^{43} ergs/sec (or 4.5×10^{36} watts) and an absolute y-magnitude of $M_y = -30.5$. This total luminosity is of the order of 10^{11} times the luminosity of the sun. However, should such temperature be attained by so large an object, the visual luminosity would also be great. An object as that described above would have about 10^{-6} of its total luminosity in the visible region, and at a distance of 3 kiloparsecs would appear to have an apparent visual magnitude, $m_v = +3.5$, thus being a clearly observable object with the naked eye. As this is clearly not the case we must conclude that the temperatures of the presently known dark globules are considerably lower than 800°K.

It is not impossible that at some stage in a possible contraction of a large globule that the total mass can attain temperatures of several hundred degrees in the closing phases of cluster formation. At such times the total energy release from the objects would rival the energy output of a supernova (about 10^{41} to 10^{42} ergs/sec) and would be observable in the infrared at a distance of over 10 megaparsecs. Therefore, if such formations do exist they may be observable in some of the nearby external galaxies.

If such large collections of matter tend to cool more rapidly than they can generate energy, or faster than energy can be fed into them, it may be difficult to detect any save the nearest examples. At temperatures around 300°K or cooler, the 8 to 14 micron detectors may prove effective.

In any case, the large surface areas of these relatively dense blobs make them prime targets for observation with infrared detectors.

CONCLUSION

It may be just possible that the observation of pre-Hertzsprung-Russel diagram protostars of the individual type might be observed in nearby young clusters using a telescope of large aperture. The answer to the question of whether a single cloud or blob could contract under its own gravitational attraction if it contained only a few solar masses of material or whether a large conglomeration of material is necessary to produce a number of protostars may provide the clue to whether any pre-stellar stage can be observed in the infrared. Indeed, observations in the longer wavelengths may provide clues to the answer to that question.

REFERENCES

1. Walker, M.F.; *Astrophys. J.* 133, 438, 1961.
2. Walker, M.F.; *Astrophys. J. Supp.* 2, 365, 1956.
3. Walker, M.F.; *Astrophys. J.* 125, 636, 1957.
4. Walker, M.F.; *Astrophys. J.* 130, 57, 1959.
5. Schwarzschild, M. "The Structure and Evolution of the Stars", P. 158
6. van de Kamp, *Pub. Ast. Soc. Pacific*, 65, 30, 1953.
7. Allen, C.W. "Astrophysical Quantities:", London 1955.
8. Johnson, M., *Astronomy of Stellar Energy and Decay* Dover, 1959, p. 142.

APPENDIX IV

REVISED IR STAR LIST INCLUDING STARS
BRIGHTER THAN $M_v = 0.0$

NOTE: Reading from left to right, the columns of the tables which follow are to be interpreted as indicated below.

Column

- 1st - IR catalog number in order of increasing Right Ascension
- 2nd, 3rd - The 1950 coordinates of the stars
- 4th - Spectral classification given in Mt. Wilson Radial Velocity Catalog
- 5th - Apparent visual magnitude given in Radial Velocity Catalog, maximum value for variable stars.
- 6th - Calculated IR index for the 2.0-2.4 micron region based upon the assumption of blackbody radiation and temperatures from the MKK spectral classification system. Brackets indicate values based on doubtful temperature assignments.
- 7th - The apparent IR magnitude in the 2.0-2.4 micron band obtained by subtracting column 6 from column 5
- 8th - Calculated IR index in the 3.2-4.2 micron band
- 9th - The apparent IR magnitude in the 3.2-4.2 micron band
- 10th - Calculated IR index in the 7.5-13.5 micron band
- 11th - The apparent IR magnitude in the 7.5-13.5 micron band
- 12th - The star designation consisting of the Radial Velocity Catalog number and the common designation

NOTES ON SELECTION

- 1) Objects were chosen for inclusion on this list which have calculated infrared apparent magnitudes, m_z (in the spectral region 7.5 to 13.5 microns), brighter than 0.0. This limit was chosen on the assumption that it represents a valid limit to the present detectability in this region using available detectors on a 60-inch telescope.
- 2) Color indices, Z.I., were calculated as a function of temperature (spectral type) assuming blackbody radiation energy distribution, and apparent visual magnitudes as listed in the Mount Wilson Radial Velocity Catalog.
- 3) The list is considered complete, except for searching errors or omissions, for stars earlier than spectral type M⁴. The search excluded all stars fainter than visual magnitude $m_V = +6.0$ due to the incompleteness of the Radial Velocity Catalog at these fainter magnitudes. The Radial Velocity Catalog was used because of the greater reliability of the spectral types given therein. Stars later than M⁴ have Z-indices greater than +6.0 and therefore withhold a substantial statistical contribution from the fainter objects on the list, but do not affect the objects brighter than -1.5 apparent z-magnitude.
- 4) From the number of objects omitted on the first search which were found on a re-examination of the Radial Velocity Catalog, it seems reasonable to conclude that there is a deficit of about 2% in the total number of objects listed; i.e., there should be expected within the limits of the survey 4 or 5 more stars, not included on the present list, plus, of course, any not included in the Radial Velocity Catalog.

No.	α 1950	δ 1950	Sp. C	μ_x	X.I.	μ_y	X.I.	μ_z	X.I.	μ_x	X.I.	μ_y	X.I.	μ_z	Star Designation
1	0 12	-8 4	G M4	5.4	5.1	+0.3	5.4	0.0	+5.8	-0.4	120	-8° 2'			
2	0 12	+19 56	G M2	4.9	4.5	+0.4	4.9	+0.0	+5.2	-0.3	122	X Per			
3	0 12	-19 13	G M1	4.7	4.2	+0.5	4.6	+0.1	+5.0	-0.3	123	7 Cet			
4	0 17	-9 06	G K3	3.8	3.4	+0.4	3.7	+0.1	+4.2	-0.4	177	4 Cet			
5	0 19	-20 20	G M5c	5.5	5.6	-0.1	5.9	-0.4	+6.2	-0.7	200	7 Cet			
6	0 25	+17 37	G M3	4.6	4.8	-0.2	5.2	-0.6	+5.5	-0.9	250	TV Per			
7	0 26	-33 17	M5	5.0	5.6	-0.6	5.8	-0.8	+5.9	-0.9	251	7 Ser			
8	0 37	+30 35	G K3	3.5	3.2	+0.3	3.8	-0.3	4.2	-0.7	357	δ And			
9	0 38	+56 16	G G7	2.5	2.3	+0.2	2.5	0.0	2.9	-0.4	344	α Cas			
10	0 41	-18 16	G O6	2.2	2.3	-0.1	2.6	-0.4	2.8	-0.6	396	β Cet			
11	0 44	+15 12	G M4	5.6	5.1	+0.5	5.5	+0.1	5.8	-0.2	427	57 Per			
12	0 52	-63 09	M5	5.6	5.6	0.0	5.9	-0.3	+5.9	-0.3	507	-63° 8'			
13	1 06	-10 27	G K1	3.6	3.0	+0.6	3.2	+0.4	3.6	0.0	660	η Cet			
14	1 07	+35 21	G M0	2.4	3.9	-1.5	4.3	-1.9	4.7	-2.3	666	β And			
15	1 35	+48 23	G M2	3.8	3.2	+0.6	3.5	+0.3	3.9	-0.1	910	51 And			
16	1 44	-51 04	M5	5.5	5.5	0.0	5.9	-0.4	5.9	-0.4	999	-51° 49'			
17	1 52	-46 33	M6	4.4	(6.0)	-1.6	(6.2)	-1.8	(6.5)	-2.1	1057	ψ Per			
18	1 58	-21 19	G M1	4.2	4.2	0.0	4.6	-0.4	5.0	-0.8	1104	U Cet			
19	1 58	-8 46	G M5	5.7	5.6	+0.1	5.9	-0.2	6.2	-0.5	1108	-9° 38'			
20	2 01	+42 05	G K3	2.3	3.4	-1.1	3.7	-1.4	4.2	-1.9	1133	γ And			
21	2 04	+23 14	G M1	2.2	2.9	-0.7	3.2	-1.0	3.6	-1.4	1160	α Ari			
22	2 17	-0 12	G M6c	2.0 max.	6.0	-4.0	6.4	-4.4	6.5	-4.5	1301	O Cet			
23	2 34	+34 3	G M4e	5.4	5.1	+0.3	5.5	-0.1	5.8	-0.4	1473	R Tri			
24	2 47	+55 41	c M4	3.9	3.5	+0.4	3.9	0.0	4.6	-0.7	1584	η Per			
25	3 00	+3 54	G M1	2.8	4.2	-1.4	4.6	-1.8	+5.2	-2.4	1688	α Cet			
26	3 02	+38 39	G M4	3.2 max.	5.1	-1.9	5.5	-2.3	5.8	-2.6	1707	ρ Per			
27	3 17	-21 56	G M3	4.0	4.7	-0.7	5.3	-1.3	5.5	-1.5	1845	τ Ser			

No.	Cl 1950	δ 1950	Sp. T	μ_V	X.I.	μ_X	Y.I.	μ_Y	Z.I.	μ_Z	Star Designation
28	3 38	+63 03	6 M4	5.3	5.2	+0.1	5.5	-0.2	5.8	-0.5	2027 +53° 597
29	3 44	-12 15	6 M2	4.6	4.4	+0.2	4.9	-0.3	5.2	-0.5	2121 π Eri
30	3 48	-74 24	M3	3.2	(4.7)	-1.5	(5.1)	-1.9	(5.5)	-2.3	2201 γ Ryl
31	3 45	+65 22	6 M1	4.7	4.2	+0.5	4.6	+0.1	5.0	-0.3	2146 +65° 349
32	3 56	-13 39	6 M0	3.2	3.9	-0.7	4.3	-1.1	4.7	-1.5	2274 γ Eri
33	3 58	-61 32	M2	4.4	(4.4)	0.0	(4.8)	-0.4	(5.2)	-0.8	2292 δ Per
34	4 00	-62 18	M5	4.5	(5.6)	-1.1	(5.9)	-1.4	(5.9)	-1.4	2304 γ Per
35	4 22	-34 8	M1	4.1	(4.2)	-0.1	(4.6)	-0.5	(5.0)	-0.9	2564 λ Eri
36	4 32	-8 20	6 M3	5.4	5.0	+0.4	5.2	+0.2	5.5	-0.1	2679 λ Eri
37	4 33	+16 25	6 M5	1.1	3.6	-2.5	3.9	-2.8	4.3	-3.2	2689 α Tau
38	4 36	-62 11	6 M7	4.5-7.0	(6.4)	-1.9	(6.5)	-2.0	(6.8)	-2.3	2726 R Dor
39	4 38	-19 46	6 M4	4.5	4.7	-0.2	5.3	-0.8	5.8	-1.3	2747 λ Eri
40	4 50	+14 10	6 M4	5.2	5.2	0.0	5.5	-0.3	5.8	-0.6	2874 θ Ori
41	4 54	+33 05	6 K3	2.9	3.4	-0.5	3.7	-0.8	4.2	-1.3	2923 λ Aur
42	4 57	-14 53	M6	5.5	(6.0)	-0.5	(6.2)	-0.7	(6.2)	-0.7	2957 R Lep
43	5 07	-63 28	M5	5.2	(5.6)	-0.4	(5.9)	-0.7	(5.9)	-0.7	3064 -63° 420
44	5 09	-11 55	6 M6	5.9	6.0	-0.1	6.2	-0.3	6.5	-0.6	3079 -11° 1092
45	5 13	+45 57	6 G1	0.2	1.9	-1.7	2.0	-1.8	2.2	-2.0	3121 α Aur
46	5 29	+18 34	c M2	4.7	4.5	+0.2	4.9	-0.2	5.3	-0.6	3354 λ Tau
47	5 48	+37 18	6 M1	5.0	4.2	+0.8	4.6	+0.4	5.0	0.0	3526 ν Aur
48	5 49	-35 47	6 M1	3.2	2.9	+0.3	3.2	0.0	3.6	-0.4	3644 β Col
49	5 52	+7 24	c M2	0.1	4.5	-4.4	4.2	-4.8	5.34	-5.24	3679 α Ori
50	5 53	+20 10	6 M8e	5.2	(6.7)	-1.5	(6.6)	-1.4	(7.1)	-1.9	3683 μ Ori
51	5 56	+45 56	6 M3	4.6	4.7	-0.1	5.1	-0.5	5.5	-0.9	3733 π Aur
52	6 11	-65 35	M4	4.9	(5.1)	-0.2	(5.5)	-0.6	(5.6)	-0.7	3930 η^2 Dor
53	6 12	+12 31	6 M3	3.1	4.7	-1.6	5.1	-2.0	5.5	-2.4	3940 η Com
54	6 13	+61 32	6 M3	5.3	4.7	+0.6	5.2	+0.1	5.5	-0.2	3962 λ Lyn

No.	α 1950	δ 1950	Sp. T	m_v	X.I.	m_x	Y.I.	m_y	Z.I.	m_z	Star Designation
55	6 20	+22 32	ε M3	3.2	4.7	-1.5	5.2	-2.0	5.5	-2.3	4046 μ Cen
56	6 30	-02 10	ε M5e	6.0	5.6	+0.4	5.9	+0.1	6.2	-0.2	4047 V Mon
57	6 23	-52 40	c F0	0.9	0.8	-1.7	0.8	-1.7	+0.8	-1.7	4091 α Car
58	6 43	-16 39	A2	-1.6	0.3	-1.9	0.3	-1.9	+0.2	-1.8	4392 α CMa
59	6 52	-24 07	c K5	4.1	4.0	+0.1	4.4	-0.3	4.7	-0.6	4521 16 CMa
60	6 55	-48 39	M3	4.9	4.7	+0.2	5.2	-0.3	5.5	-0.6	4568 -18° 2601
61	7 00	-51 20	M3	5.0	4.7	+0.3	5.2	-0.2	5.5	-0.5	4621 -51° 2224
62	7 00	-27 52	c M0	3.7	4.2	-0.5	4.6	-0.9	5.0	-1.2	4625 σ CMa
63	7 06	-26 19	c G3	2.0	2.4	-0.4	2.6	-0.6	3.0	-1.0	4704 δ CMa
64	7 12	-44 33	M5e	3.4	5.6	-2.2	5.9	-2.5	6.2	-2.8	4782 12 Pup
65	7 15	-27 47	ε M3	4.8	4.7	+0.1	5.2	-0.4	5.5	-0.7	4914 -27° 3522
66	7 15	-37 00	K5	2.7	2.5	+0.2	2.7	0.0	3.1	-0.4	4825 π Pup
67	7 21	+82 31	ε M4	4.7	5.1	-0.4	5.5	-0.8	5.8	-1.1	4776 ν 2 Cen
68	7 28	-43 12	M0	3.3	(3.9)	-0.6	(4.3)	-1.0	(4.7)	-1.4	5001 σ Pup
69	7 32	+14 25	ε M3ep	5.1	4.7	+0.4	5.2	+0.1	5.5	-0.4	5045 -24° 1971
70	7 33	+27 01	ε M0	4.2	3.9	+0.3	4.3	-0.1	4.7	-0.5	5040 ν Cen
71	7 37	+5 21	d F3	0.5	1.0	-0.5	1.0	-0.5	1.0	-0.5	5077 α CMi
72	7 42	+28 09	ε G8	1.2	2.5	-1.3	2.7	-1.5	3.0	-1.8	5166 β Cen
73	7 43	+37 38	ε M3	5.4	4.7	+0.7	5.2	+0.2	5.5	-0.1	5173 +37° 1749
74	7 59	-60 27	M3	5.1	4.7	+0.4	5.2	-0.1	5.5	-0.4	5339 -60° 1018
75	8 02	-32 32	M4	5.4	5.6	-0.2	5.9	-0.5	5.8	-0.4	5368 -32° 4796
76	8 10	-39 28	M0	4.4	3.9	+0.5	4.3	+0.1	4.7	-0.3	5434 -39° 4084
77	8 22	-59 21	K0	1.7	2.0	-0.3	2.0	-0.3	2.2	-0.5	5546 ϵ Car
78	8 22	-77 19	K5	4.3	3.6	+0.7	3.9	+0.4	4.3	0.0	5555 θ Cha
79	8 58	+67 50	ε M3	5.0	4.7	+0.3	5.2	-0.2	5.5	-0.5	5918 ρ UMa
80	9 06	-43 14	c M4	2.2	3.9	-1.7	4.2	-2.0	4.6	-2.4	5989 λ Vel
81	9 08	+31 10	ε M5	5.5	6.0	-0.5	6.2	-0.7	6.5	-1.0	6007 ν 5 Cen

No.	Cl 1950	δ 1950	Sp. T	μ_V	X.I.	μ_X	Y.I.	μ_Y	Z.I.	μ_Z	Star Designation
82	9 14	-44 03	M2	5.0	4.4	+0.6	4.9	+0.1	5.2	-0.2	6055
83	9 15	-57 20	K5	4.2	3.5	+0.7	3.9	+0.3	4.3	-0.1	6058
84	9 19	-25 45	K M1	4.9	4.2	+0.7	4.6	+0.3	5.0	-0.1	6095
85	9 25	-8 26	K K5	2.2	3.5	-1.3	3.9	-1.7	4.3	-2.1	6136
86	9 27	-35 44	M0	4.6	3.9	+0.7	4.3	+0.3	4.7	-0.1	6150
87	9 31	-62 31	K M5c	5.6	5.6	0.0	5.9	-0.3	6.2	-0.6	6189
88	9 43	+34 45	K M8e	6.0	(6.7)	-0.7	(7.0)	-1.0	(7.1)	-1.1	6269
89	9 43	+57 22	K M3	5.4	4.7	+0.7	5.1	+0.3	5.5	-0.1	6273
90	9 45	+11 40	K M8e	4.4	(6.7)	-2.3	(6.9)	-2.5	(7.1)	-2.7	6288
91	9 50	+26 15	K K3	4.1	3.4	+0.7	3.7	+0.4	4.2	-0.1	6325
92	9 58	+8 17	K M2	4.9	4.4	+0.5	4.9	0.0	5.2	-0.3	6375
93	10 17	+20 06	K K1	2.6	2.9	-0.3	3.2	-0.6	3.6	-1.0	6502
94	10 25	-30 49	M0	4.4	(3.9)	+0.5	(4.3)	+0.1	(4.7)	-0.3	6563
95	10 30	-72 58	M1	4.9	4.2	+0.7	4.6	+0.3	5.0	-0.1	6601
96	10 35	-27 09	K M2	5.1	4.5	+0.6	4.9	+0.2	5.2	-0.1	6629
97	10 35	-78 21	M0	4.1	(3.9)	+0.2	(4.3)	-0.2	(4.7)	-0.6	6630
98	10 37	-58 55	M1	4.8	4.2	+0.6	4.6	+0.2	5.0	-0.2	6642
99	10 42	-60 18	M1	4.5	4.2	+0.3	4.6	-0.1	5.0	-0.5	6683
100	10 47	-15 56	K K3	3.3	3.4	-0.1	3.7	-0.4	4.2	-0.9	6726
101	10 53	+6 27	K M5	6.0	5.6	+0.4	5.9	+0.1	6.2	-0.2	6772
102	10 59	-2 13	K M1	5.0	4.2	+0.8	4.6	+0.4	5.0	0.0	6812
103	11 01	+6 21	K G7	2.0	2.4	-0.4	2.6	-0.6	2.9	-0.9	6819
104	11 07	+44 46	K K1	3.2	3.0	+0.2	3.2	0.0	3.6	-0.4	6861
105	11 12	+23 22	K M2	4.9	4.4	+0.5	4.9	0.0	5.2	-0.3	6901
106	11 16	+33 22	K K3	3.7	3.4	+0.3	3.7	0.0	4.2	-0.5	6924
107	11 28	+69 36	K M0	4.1	3.9	+0.2	4.3	-0.2	4.7	-0.6	7012
108	11 30	-30 49	M2	5.2	4.4	+0.6	4.9	+0.3	5.2	0.0	7027

No.	α 1950	δ 1950	Sp. T	m_v	X.I.	m_x	Y.I.	m_y	Z.I.	m_z	Star Designation
109	11 36	+8 25	K M6	5.5	6.0	-0.5	6.2	-0.7	6.5	-1.0	7072 G1 V1r
110	11 43	+6 49	K M1	4.2	4.2	0.0	4.6	-0.4	5.0	-0.8	7128 V V1r
111	11 46	-66 32	M2	4.7	4.4	+0.3	4.9	-0.2	5.2	-0.5	7142 μ Mus
112	11 46	-26 28	K M4	5.4	5.2	+0.2	5.5	-0.1	5.8	-0.4	7147 -86° 8789
113	12 08	-22 21	K M3	3.5	3.4	-0.2	3.7	-0.5	4.2	-1.0	7289 ϵ Crv
114	12 15	-67 41	M5 M6	4.5	(6.0)	-1.8	(6.2)	-2.0	(+6.3)	-2.1	7353 ϵ Mus
115	12 17	-18 59	K M5e	5.9	5.6	+0.3	5.9	0.0	6.2	-0.1	7389 ρ Crv
116	12 25	-58 43	M6	5.4	(6.0)	-0.6	(6.2)	-0.8	(6.5)	-1.1	7482 -98° 4289
117	12 28	+69 29	K M4	5.2	5.2	0.0	5.5	-0.3	5.8	-0.6	7523 λ Dm
118	12 28	-56 50	M4	1.6	5.2	-3.6	5.5	-3.9	5.8	-4.2	7528 γ Crv
119	12 52	-9 15	K M3	4.9	4.7	-0.2	5.1	-0.2	5.5	-0.6	7720 ψ V1r
120	12 53	-47 28	c M8	6.0	(6.7)	-0.7	(6.9)	-0.9	(7.3)	-1.3	7724 TU Crv
121	12 53	+5 47	K M3	3.7	4.7	-1.0	5.2	-1.4	5.5	-1.8	7728 β V1r
122	13 4	+22 53	M5 M5	5.9	(5.6)	+0.3	(5.9)	0.0	(6.0)	-0.1	7801 λ 0 Com
123	13 15	+5 49	K M2	5.0	4.4	-0.6	4.9	-0.1	5.2	-0.2	7902 σ V1r
124	13 27	-23 01	K M7e	3.5	(6.4)	-2.9	(6.6)	-3.1	(6.8)	-3.3	8006 ρ Dm
125	13 29	-6 0	K M3	4.8	4.7	+0.1	5.1	-0.3	5.5	-0.7	8020 η V1r
126	13 30	-6 56	K M7e	6.0	6.4	-0.4	6.6	-0.6	6.8	-0.8	8027 β V1r
127	13 39	-8 27	K M2	5.2	4.4	+0.8	4.9	+0.3	5.2	0.0	8095 δ V1r
128	13 39	+54 56	K M2	4.8	4.4	+0.4	4.9	-0.1	5.2	-0.4	8093 δ 3 UMa
129	13 46	-34 12	M5 M5	4.4	(6.0)	-1.6	(6.2)	-1.8	(6.3)	-1.9	8152 α Com
130	13 47	+16 03	K M0	4.3	3.9	+0.4	4.3	0.0	4.7	-0.4	8159 V Boo
131	13 50	+64 58	K M3	4.8	4.7	+0.1	5.1	-0.3	5.5	-0.7	8189 λ 0 Dm
132	13 50	+34 41	K M2	5.0	4.4	+0.6	4.9	+0.1	5.2	-0.2	8184 +34° 2446
133	14 04	-26 27	K M3	3.5	3.4	+0.1	3.7	-0.2	4.2	-0.7	8270 η Dm
134	14 04	-36 07	K 69	2.3	(2.6)	-2.5	(2.8)	-2.7	3.2	-0.9	8272 θ Com
135	14 08	-16 4	K M3	5.1	4.7	+0.4	5.1	0.0	5.5	-0.4	8300 -15° 3817

No.	Q 1950	δ 1950	Sp. T	μ_x	X.I.	μ_y	Y.I.	μ_z	Z.I.	μ_z	Star Designation
136	14 13	+19 27	K K0	0.2	5.0	-4.8	2.9	-2.7	+3.4	-3.2	B341
137	14 30	+30 35	K K3	3.8	3.4	+0.4	3.7	+0.1	4.2	-0.4	B475
138	14 36	-60 38	d G4	0.1	(1.6)	-1.5	(1.6)	-1.5	(+1.8)	-1.7	B517
139	14 41	+26 44	K M3	4.9	4.7	+0.2	5.3	-0.4	5.5	-0.6	B555
140	14 43	+27 17	K K0	2.7	2.7	0.0	2.9	-0.2	3.4	-0.7	B567
141	14 51	+74 22	K K5	2.2	3.6	-1.4	3.9	-1.7	4.3	-2.1	B5A7
142	14 57	+66 8	K M5	4.9	5.6	-0.7	5.9	-1.0	6.2	-1.3	B5B9
143	15 1	-25 5	K M4	3.4	5.1	-1.7	5.5	-2.1	5.7	-2.3	B717
144	15 19	+31 33	K M7c	5.8	(6.4)	-0.6	(6.5)	-0.7	(6.8)	-1.0	B890
145	15 24	+59 08	K K3	3.5	3.4	+0.1	3.7	-0.2	4.2	-0.7	B925
146	15 34	-27 58	K K5	3.8	3.6	+0.2	3.9	-0.1	4.3	-0.5	9005
147	15 35	-42 24	M0	4.3	3.5	+0.8	3.8	+0.5	4.7	-0.4	9016
148	15 42	+6 35	K M2	2.8	3.2	-0.4	3.5	-0.7	3.4	-0.6	9079
149	15 53	+43 17	K K3	5.5	(4.7)	+0.8	(5.1)	+0.4	(5.5)	0.0	9163
150	15 57	+26 04	Q+E M3	2.0	4.7	-2.7	5.1	-3.1	5.5	-3.5	9203
151	15 12	-3 34	K M0	3.0	3.9	-0.9	4.3	-1.3	4.7	-1.7	9340
152	16 13	-53 14	M3	5.4	4.7	+0.7	5.1	+0.3	5.5	-0.1	9349
153	16 13	-78 39	M5	4.8	(5.6)	-0.8	(6.2)	-1.4	(6.2)	-1.4	9350
154	16 16	+59 53	K M4	5.6	5.1	+0.5	5.5	+0.1	5.8	-0.2	9392
155	16 26	-26 19	c M1	1.2	4.2	-3.0	4.6	-3.4	-5.2	-4.0	9479
156	16 27	+41 59	K M6	5.0	6.0	-1.0	6.2	-1.2	6.5	-1.5	9485
157	16 33	-35 9	M4	4.3	3.9	+0.4	4.3	0.0	4.7	-0.4	9541
158	16 37	+49 2	K M2	5.1	4.4	+0.7	4.8	+0.3	5.2	-0.1	9575
159	16 43	-68 56	K5	1.9	3.6	-1.7	3.9	-2.0	4.3	-2.4	9640
160	16 47	-34 12	K O9	2.4	2.5	-0.1	2.7	-0.3	3.2	-0.8	9669
161	16 50	+15 01	K M5c	5.9	5.6	+0.3	5.9	0.0	6.2	-0.3	9666
162	16 51	-42 17	K K5	3.8	3.6	+0.2	3.9	-0.1	4.3	-0.5	9719

No.	α 1950	δ 1950	Sp. T	m_v	X.I.	m_x	Y.I.	m_y	Z.I.	m_z	Star Designation
163	16 52	-45 01	G M6e	6.0	6.0	0.0	6.2	-0.2	6.5	-0.5	9735
164	16 53	-30 30	G M6e	5.0	6.0	-1.0	6.3	-1.3	6.5	-1.5	9756
165	16 56	-53 05	M1	4.2	4.2	0.0	4.6	-0.4	5.0	-0.8	9777
166	17 01	+14 10	G M3	5.1	3.8	+1.3	4.2	+0.9	5.5	-0.4	5831
167	17 12	+14 27	G M5	3.5	5.6	-2.1	5.9	-2.4	6.5	-3.0	5944
168	17 13	+36 52	G K5	3.4	3.6	-0.2	3.9	-0.5	4.3	-0.9	5955
169	17 41	+4 35	G K1	2.9	2.9	0.0	3.2	-0.3	3.6	-0.7	10,239
170	17 54	-41 43	M1	4.9	3.8	+1.1	4.2	+0.7	5.0	-0.1	10,380
171	17 54	+37 15	c K1	4.0	3.3	+0.7	3.7	+0.3	4.1	-0.1	10,385
172	17 55	+51 30	G K5	2.4	3.6	-1.2	3.9	-1.5	4.3	-1.9	10,394
173	18 10	+31 23	G M3	5.0	4.7	+0.3	5.1	-0.1	5.5	-0.5	10,658
174	18 14	-36 47	G M4	3.2	5.1	-1.9	5.5	-2.3	5.8	-2.6	10,737
175	18 18	-29 51	G K2	2.8	3.2	-0.4	3.5	-0.7	3.9	-1.1	10,810
176	18 19	-61 31	M1	4.2	3.8	+0.4	4.2	0.0	5.0	-0.8	10,823
177	18 20	+49 6	G M2	5.1	4.4	+0.7	4.9	+0.2	5.2	-0.1	10,854
178	18 25	-25 27	G K1	2.9	2.2	0.0	3.1	-0.2	3.6	-0.7	10,927
179	18 32	-8 17	G K5	4.1	3.5	+0.6	3.9	+0.2	4.1	-0.2	11,039
180	18 36	+8 47	G M6e	5.9	6.2	-0.1	6.2	-0.3	6.5	-0.6	11,092
181	18 36	-43 14	M4	5.4	5.1	+0.3	5.5	-0.1	5.8	-0.4	11,093
182	18 53	+43 53	G M5	4.0	5.6	-1.6	5.9	-1.9	6.2	-2.2	11,388
183	18 53	+36 50	G M4	4.5	5.1	-0.6	5.5	-1.0	5.8	-1.3	11,399
184	18 55	-21 10	G K1	3.6	3.0	+0.6	3.2	+0.4	3.6	0.0	11,399
185	19 04	-27 45	G K1	3.4	3.0	-0.4	3.2	-0.2	3.6	-0.2	11,558
186	19 04	+8 09	G M7e	5.1	(6.4)	-1.3	(6.6)	-1.5	(6.8)	-1.7	11,562
187	19 27	+24 34	G M1	4.6	4.2	+0.4	4.6	0.0	5.0	-0.4	11,909
188	19 44	+10 29	G M4	2.8	3.5	-0.7	3.8	-1.0	4.3	-1.5	12,137
189	19 45	+18 25	G M2	3.8	4.4	-0.6	4.8	-1.0	5.2	-1.4	12,160

No.	Q 1950	δ 1950	Sp. T	μ_y	X.I.	μ_x	Y.I.	μ_y	Z.I.	μ_z	Star Designation
190	19 49	+32 47	g M7e	2.3	(6.4)	-4.1	(6.6)	-4.3	(6.8)	-4.5	X CVR
191	19 53	-29 20	g M5e	5.5	5.6	-0.1	5.9	-0.4	6.2	-0.7	RR Sgr
192	19 56	+19 21	g M0	3.7	3.9	-0.2	4.3	-0.6	4.7	-1.0	γ Sgr
193	19 58	-59 31	M5	5.1	6.0	-0.9	6.2	-1.1	6.5	-1.4	-59° 75A
194	19 58	+17 23	g M4	5.6	5.1	+0.5	5.5	+0.1	5.8	-0.2	13 Sgr
195	20 00	-27 51	g M4	4.6	5.1	-0.5	5.5	-0.9	5.8	-2.2	62 Sgr
196	20 12	+46 35	c M1	4.0	2.5	+1.5	2.6	+1.4	4.1	-0.1	O CVR
197	20 14	+47 34	c K5	4.2	4.0	+0.2	4.4	-0.2	4.7	-0.5	32 CVR
198	20 43	17 54	c M5	5.6	(6.0)	-0.4	(6.2)	-0.6	(6.8)	-1.2	U Del
199	20 44	+33 47	g K0	2.6	2.7	-0.1	2.9	-0.3	3.4	-0.8	13,020
200	20 45	-5 13	g M3	4.6	4.7	-0.1	5.2	-0.6	5.5	-0.9	13,035
201	20 46	-46 25	M1	4.9	3.8	+1.1	4.2	+0.7	5.0	-0.1	13,052
202	20 49	-27 6	g M1	4.2	4.2	0.0	4.6	-0.4	5.0	-0.8	13,085
203	20 51	-58 39	M2	3.7	2.2	+1.5	2.4	+1.3	3.9	-0.2	13,108
204	21 04	-25 12	g M1	4.6	4.2	+0.4	4.6	0.0	5.0	-0.4	13,266
205	21 09	-70 20	M2	5.1	4.2	+0.9	4.6	+0.5	5.2	-0.1	13,315
206	21 09	+68 17	g M7e	5.5	(6.4)	-0.9	(6.6)	-1.1	(6.8)	-1.3	13,330
207	21 13	-15 23	g M3	5.5	4.7	+0.8	5.1	+0.4	5.5	0.0	13,361
208	21 24	-59 43	M5	5.5	6.0	-0.5	6.2	-0.7	6.5	-1.0	13,486
209	21 28	+23 25	g M1	4.8	4.2	+0.6	4.6	+0.2	5.0	-0.2	13,515
210	21 34	+45 09	g M4e	5.0	5.1	-0.1	5.5	-0.5	5.8	-0.8	13,572
211	21 42	+9 39	c K0	2.5	3.2	-0.7	3.5	-1.0	3.4	-0.9	13,654
212	21 42	+58 33	c M2e	3.6	4.5	-0.9	4.9	-1.3	5.3	-1.7	13,658
213	22 02	+62 53	g M5	5.5	5.6	-0.1	5.9	-0.4	6.2	-0.7	13,871
214	22 03	-39 47	M0	4.6	3.5	+1.1	3.8	+0.8	4.7	-0.1	13,877
215	22 06	-34 17	M2	5.1	4.2	+0.9	4.6	+0.5	5.2	-0.1	13,908
216	22 09	+57 57	c K5	3.6	4.0	-0.4	4.4	-0.8	4.7	-1.1	13,949

APPENDIX V

SUMMARY OF STELLAR MEASUREMENTS AT PERKINS OBSERVATORY

SUMMARY OF STELLAR MEASUREMENTS AT PERKINS OBSERVATORY
1 JULY 1960 TO 31 DECEMBER 1960

Star Designation		Sp. T	m _v	m _x	XI	H _γ (watts/cm ²)	m _y	YI	H _γ (watts/cm ²)
IR No.	Name								
20	γ And	G K3	+2.3	-1.0	3.3	5 x 10 ⁻¹⁵	-0.4	2.7	1.2 x 10 ⁻¹⁵
21	α Ari	G K1	+2.2				+0.3	1.9	2.2 x 10 ⁻¹⁶
22	ο Cet	G M6e	*	-3.0	*	3.2 x 10 ⁻¹⁴	-3.5	*	7.5 x 10 ⁻¹⁵
25	α Cet	G M2	+2.8	-1.7	4.5	10 ⁻¹⁴	-1.4	4.2	1.2 x 10 ⁻¹⁵
26	ρ Per	G M4	+3.5	-1.9	5.4	1.2 x 10 ⁻¹⁴	-2.1	5.6	2 x 10 ⁻¹⁵
37	α Tau	G K5	+1.1	-2.9	4.0	3 x 10 ⁻¹⁴	-2.9	4.0	4.8 x 10 ⁻¹⁵
41	ι Aur	G K3	+2.9	-0.4	3.3	3 x 10 ⁻¹⁵			
45	α Aur	G K1	+0.2	-1.7	1.9	10 ⁻¹⁴	-2.2	2.4	2.3 x 10 ⁻¹⁵
49	α Ori	c M2	+0.1	-4.6	4.7	1.4 x 10 ⁻¹³	-5.0	5.1	3 x 10 ⁻¹⁴
50	υ Ori	G M8e	+11.3				-0.8	12.1	7 x 10 ⁻¹⁶
53	η Gem	G M3	+3.1	-1.3	4.4	7 x 10 ⁻¹⁵	-1.2	3.3	9 x 10 ⁻¹⁶
55	μ Gem	G M3	+3.2	-2.0	5.2	1.3 x 10 ⁻¹⁴	-1.8	4.0	1.8 x 10 ⁻¹⁵
58	α CMa	A2	-1.4	-1.3	-0.1	7 x 10 ⁻¹⁵	-0.6	-0.8	5 x 10 ⁻¹⁶
	R Lyn	S3,9e	9.0				+1.9	7.1	5 x 10 ⁻¹⁷

**SUMMARY OF STELLAR MEASUREMENTS AT PERKINS OBSERVATORY
1 JULY 1960 TO 31 DECEMBER 1960**

Star Designation		Sp. T	m_x	m_y	m_z	XI	B_x (watts/cm ²)	m_y	YI	B_y (watts/cm ²)
IR No.	Name									
136	α Boo	G K0	+0.2	-2.2	2.4	1.5×10^{-14}				
167	α Her	G M5	+3.5	-3.5	7.0	5×10^{-14}				
	α Lyr		0.0	0.0	0.0					
186	R Aql	G M7e	+8.3	-0.8	9.1	4.5×10^{-15}				
188	γ Aql	G K4	+2.8	+0.1	2.7	1.8×10^{-15}				
190	χ Cyg	G M7e	+5.3	-2.3	7.6	1.8×10^{-14}				
198	U Del	c M6	+5.6	-0.9	6.5	4.8×10^{-15}				
206	T Cep	G M7e	+6.4	-1.7	8.1	10^{-14}		-2.1	8.5	2×10^{-15}
212	μ Cep	c M2e	+3.6	-2.1	5.7	1.4×10^{-14}				
216	ζ Cep	c K5	+3.6	0.0	3.6	2×10^{-15}				
225	β Peg	G M2	+2.6	-2.3	4.9	1.8×10^{-14}		-2.0	4.6	1.9×10^{-15}
231	η Peg	G M5	+5.5	-0.4	5.9	3×10^{-15}				
235	R Cas	G M7e	+4.8	-1.8	6.6	1.2×10^{-14}				
9	α Cas	G G7	+2.5	+0.1	2.4	1.8×10^{-15}		-0.3	2.8	4×10^{-16}
14	β And	G M0	+2.4	-2.0	4.4	1.3×10^{-15}		-1.6	4.0	1.3×10^{-15}

DISTRIBUTION LIST

	<u>COPY</u>		<u>COPY</u>
Commander Army Rocket and Guided Missile Agency Redstone Arsenal, Alabama ATTN: CROSD-DRP CROSD-DRB CROSD-DRL CROSD-DRP CROSD-DRK	1-4 5-13 14-15 16 17	Hughes Aircraft Company Building 5, Mail Station 1810 Culver City, California ATTN: Mr. C. F. Arnold	2
Contracting Officer New York Ordnance District 770 Broadway, New York 2, N.Y. ATTN: CROSD-O-CA, Contracting Officer	18	Jet Propulsion Laboratory California Institute of Technology 4800 Oak Grove Drive Pasadena, California ATTN: Technical Library	3
Aerajet-General Corporation Azusa, California ATTN: Mr. B. W. Powell	19	MIT Lincoln Laboratory Box 7J Lexington 73, Massachusetts ATTN: D. E. Dustin	3
Aerodynamics A Division of Ford Motor Company Ford Road, Dearborn Beach, California ATTN: Library	20	Radio Corporation of America Moorestown, New Jersey ATTN: Mr. Moltzop	3
Johns Hopkins University Applied Physics Laboratory 8211 Georgia Avenue Silver Spring, Maryland ATTN: Mr. A. C. Schultze	21	Raytheon Manufacturing Company Missile and Radar Division-Advanced Development Section Bedford, Massachusetts ATTN: Mr. Harold Soule	3
Armour Research Foundation 10 W. 35th Street Chicago 16, Illinois ATTN: T. Paul Torde, Director Fluid Dynamics and Propulsion Research	22	Space Technology Laboratories, Inc. P.O. Box 95001 Los Angeles 45, California ATTN: Technical Information Center Document Procurement Bldg. C Room 2412	3
ATCO Research Laboratory 2385 Revere Beach Parkway Everett 49, Massachusetts ATTN: Dr. C. Petty	23	Stanford Research Institute Menlo Park, California ATTN: Dr. Schuch	3
Larnes Engineering Company 30 Commerce Road Stamford, Connecticut ATTN: Mr. Harold Yates	24	Sylvania Electric Products, Inc. 100 First Avenue Waltham 54, Massachusetts ATTN: Library	3
Bell Telephone Laboratories, Inc. Whippany Road Whippany, New Jersey ATTN: Library	25	Commanding Officer Electronics Research Directorate Air Force Cambridge Research Center L. G. Hanscom Field Bedford, Massachusetts ATTN: CHR	3
Bendix Corporation Bendix Systems Division 3300 Plymouth Road Ann Arbor, Michigan ATTN: Mr. W. Bartz	26	Commander Air Research and Development Command Andrews Air Force Base Washington 25, D. C. ATTN: RDZEB RDRMF RDAME	3 3 4
Convair Division of General Dynamics San Diego, California ATTN: Dr. Heinz Pappendick	27	Chief, ARDC Office Room C-107, Building 448C Redstone Arsenal, Alabama	4
Cornell Aeronautical Laboratory 4455 Genesee Street Buffalo 21, New York ATTN: Library	28	Commander Army Rocket and Guided Missile Agency Redstone Arsenal, Alabama ATTN: Technical Library	4

DISTRIBUTION LIST - CONT.

Commanding General U. S. Army Signal Research and Development Laboratory, Ft. Monmouth, New Jersey ATTN: SIDA/SL-37	58	Commanding General U. S. Army Signal Research and Development Laboratory, Ft. Monmouth, New Jersey ATTN: SIDA/SL-37	59
Commanding Officer Ballistics Research Laboratory Aberdeen Proving Ground, Maryland ATTN: Dr. B. B. Smith	60	Commanding Officer Ballistics Research Laboratory Aberdeen Proving Ground, Maryland ATTN: Dr. B. B. Smith	60
Central Intelligence Agency 2430 E. Street S. W. Washington 25, D. C. ATTN: CCR Branch - Specialized	60	Central Intelligence Agency 2430 E. Street S. W. Washington 25, D. C. ATTN: CCR Branch - Specialized	61
Chief of Ordnance Department of the Army Washington 25, D. C. ATTN: OBRV	61	Chief of Ordnance Department of the Army Washington 25, D. C. ATTN: OBRV	61
Chief of Naval Operations Department of the Navy Washington 25, D. C. ATTN: OP-677	61	Chief of Naval Operations Department of the Navy Washington 25, D. C. ATTN: OP-677	61
Commanding Officer Directed Ordnance Fuse Laboratories Washington 25, D. C. ATTN: Technical Services Branch OBRV-212 OBRV-210	61 62	Commanding Officer Directed Ordnance Fuse Laboratories Washington 25, D. C. ATTN: Technical Services Branch OBRV-212 OBRV-210	62 62
Commanding Officer Naval Research Laboratory Washington 25, D. C. ATTN: 5305 NRL (Two Naval Attaches)	62 63	Commanding Officer Naval Research Laboratory Washington 25, D. C. ATTN: 5305 NRL (Two Naval Attaches)	63 64
Director of Electronic Office of the Assistant Secretary of Defense Research and Engineering Washington 25, D. C. ATTN: James H. Hodge	64	Director of Electronic Office of the Assistant Secretary of Defense Research and Engineering Washington 25, D. C. ATTN: James H. Hodge	64
Commanding Officer Ordnance Technical Intelligence Agency Arlington Hall Station Arlington 12, Virginia ATTN: Major V. Love	65	Commanding Officer Ordnance Technical Intelligence Agency Arlington Hall Station Arlington 12, Virginia ATTN: Major V. Love	65
Headquarters Rome Air Development Center Griffiss Air Force Base, New York ATTN: RCEM, Directorate of Research and Ordnance RCEM, Joel S. Greenberg, Advanced Studies Office, DTR/Research	66 67	Headquarters Rome Air Development Center Griffiss Air Force Base, New York ATTN: RCEM, Directorate of Research and Ordnance RCEM, Joel S. Greenberg, Advanced Studies Office, DTR/Research	67 68
Geophysics Corporation of America 700 Commonwealth Avenue Boston 15, Massachusetts ATTN: Mr. Richard Ows	68	Geophysics Corporation of America 700 Commonwealth Avenue Boston 15, Massachusetts ATTN: Mr. Richard Ows	68
Director of Special Projects Department of the Navy Washington 25, D. C. ATTN: Mr. V. F. Baber Dr. Ralph Linstead	69 70	Director of Special Projects Department of the Navy Washington 25, D. C. ATTN: Mr. V. F. Baber Dr. Ralph Linstead	69 70
		Commanding General U. S. Army Signal Research and Development Laboratory, Ft. Monmouth, New Jersey ATTN: SIDA/SL-37	71
		Commanding Officer Ballistics Research Laboratory Aberdeen Proving Ground, Maryland ATTN: Dr. B. B. Smith	72
		Central Intelligence Agency 2430 E. Street S. W. Washington 25, D. C. ATTN: CCR Branch - Specialized	73
		Chief of Ordnance Department of the Army Washington 25, D. C. ATTN: OBRV	74
		Chief of Naval Operations Department of the Navy Washington 25, D. C. ATTN: OP-677	75
		Commanding Officer Directed Ordnance Fuse Laboratories Washington 25, D. C. ATTN: Technical Services Branch OBRV-212 OBRV-210	76
		Commanding Officer Naval Research Laboratory Washington 25, D. C. ATTN: 5305 NRL (Two Naval Attaches)	77
		Director of Electronic Office of the Assistant Secretary of Defense Research and Engineering Washington 25, D. C. ATTN: James H. Hodge	78
		Commanding Officer Ordnance Technical Intelligence Agency Arlington Hall Station Arlington 12, Virginia ATTN: Major V. Love	79
		Headquarters Rome Air Development Center Griffiss Air Force Base, New York ATTN: RCEM, Directorate of Research and Ordnance RCEM, Joel S. Greenberg, Advanced Studies Office, DTR/Research	80
		Geophysics Corporation of America 700 Commonwealth Avenue Boston 15, Massachusetts ATTN: Mr. Richard Ows	81
		Director of Special Projects Department of the Navy Washington 25, D. C. ATTN: Mr. V. F. Baber Dr. Ralph Linstead	82
		Commanding General U. S. Army Signal Research and Development Laboratory, Ft. Monmouth, New Jersey ATTN: SIDA/SL-37	83
		Commanding Officer Ballistics Research Laboratory Aberdeen Proving Ground, Maryland ATTN: Dr. B. B. Smith	84
		Central Intelligence Agency 2430 E. Street S. W. Washington 25, D. C. ATTN: CCR Branch - Specialized	85
		Chief of Ordnance Department of the Army Washington 25, D. C. ATTN: OBRV	86
		Chief of Naval Operations Department of the Navy Washington 25, D. C. ATTN: OP-677	87
		Commanding Officer Directed Ordnance Fuse Laboratories Washington 25, D. C. ATTN: Technical Services Branch OBRV-212 OBRV-210	88
		Commanding Officer Naval Research Laboratory Washington 25, D. C. ATTN: 5305 NRL (Two Naval Attaches)	89
		Director of Electronic Office of the Assistant Secretary of Defense Research and Engineering Washington 25, D. C. ATTN: James H. Hodge	90
		Commanding Officer Ordnance Technical Intelligence Agency Arlington Hall Station Arlington 12, Virginia ATTN: Major V. Love	91
		Headquarters Rome Air Development Center Griffiss Air Force Base, New York ATTN: RCEM, Directorate of Research and Ordnance RCEM, Joel S. Greenberg, Advanced Studies Office, DTR/Research	92
		Geophysics Corporation of America 700 Commonwealth Avenue Boston 15, Massachusetts ATTN: Mr. Richard Ows	93
		Director of Special Projects Department of the Navy Washington 25, D. C. ATTN: Mr. V. F. Baber Dr. Ralph Linstead	94
		Commanding General U. S. Army Signal Research and Development Laboratory, Ft. Monmouth, New Jersey ATTN: SIDA/SL-37	95
		Commanding Officer Ballistics Research Laboratory Aberdeen Proving Ground, Maryland ATTN: Dr. B. B. Smith	96
		Central Intelligence Agency 2430 E. Street S. W. Washington 25, D. C. ATTN: CCR Branch - Specialized	97
		Chief of Ordnance Department of the Army Washington 25, D. C. ATTN: OBRV	98
		Chief of Naval Operations Department of the Navy Washington 25, D. C. ATTN: OP-677	99
		Commanding Officer Directed Ordnance Fuse Laboratories Washington 25, D. C. ATTN: Technical Services Branch OBRV-212 OBRV-210	100

71-72-73

74

DISTRIBUTION LIST - CONT'D

	<u>COPY</u>	
Director Langley Research Center National Aeronautics and Space Administration Langley Field, Virginia ATTN: Library	75	Foreign Technology Division Wright-Patterson Air Force Base Ohio ATTN: TD-81a
National Aeronautics and Space Administration Lewis Research Center 2100 Brookpark Road Cleveland 15, Ohio ATTN: Library	76	Rand Corporation 1000 Connecticut Avenue, N.W. Washington 6, D. C.
Electro-Optical Systems, Incorporated Advanced Electronics and Information Systems Division 125 N. Vinado Avenue Pasadena, California ATTN: Mr. Henry J. Richter, Jr.	77	Commander Air Force Cambridge Research Laboratory Air Force Research Division Lawrence G. Hanscom Field Bedford, Massachusetts ATTN: CPOC, Mr. T. C. Goodson
General Electric Company P. O. Box 459 Utica, New York ATTN: Technical Information Center	78	Armed Services Technical Information Agency Arlington Hall Station Arlington 12, Virginia
Manchester University Department of Astronomy Manchester, England	79	Kastman Kodak Company Apparatus and Optical Division Rochester, New York Mr. V. Forman Dr. F. C. E. Odeh Mr. I. Geese Mr. P. Erlagard Mr. C. F. Crum Dr. W. E. Raynie Mr. A. Prusil File Center, Lincoln Post 100-22 (plus one reproducible)

UNCLASSIFIED

UNCLASSIFIED